DETERMINATION OF AIRPLANE LONGITUDINAL STABILITY DERIVATIVES FROM TRANSIENT RESPONSES

S. M. COOLEY, JR.
F. S. PETERSEN
J. F. IRVINE, JR.

DETERMINATION OF AIRPLANE LONGITUDINAL STABILITY DERIVATIVES FROM TRANSIENT RESPONSES

S. M. Cooley, Jr., Lt. USN
F. S. Petersen, Lt. USN
J. F. Irvine, Jr., Lt. USN

Aeronautical Engineering Report No. 231

June 1, 1953

Submitted in partial fulfillment of the requirements for the degree of Master of Science in Engineering from Princeton University, 1953.

ACKNOWLEDGMENT

The authors are indebted to Professors C. D. Perkins and E. Seckel under whose supervision this project was performed. They have given freely of their time, and their helpful discussions have been invaluable as the project progressed.

Gratitude is also expressed to Mr. Harry Williams for his aid in the initial instrumentation and in instrument trouble shooting; to Mr. Robert Cooper, airport manager, for his cooperation and aid in many minor crises; to Mr. Harry Ashworth for his extreme cooperation in instrument installation; and to the Naval Air Test Center, Patuxent River, Maryland for the use of equipment in the Flight Test Instrumentation Section for gyro calibration.

The authors are especially grateful to the Aeronautical Engineering Department of Princeton University for the use of their aircraft and flight test facilities. Without their progressive outlook and their excellent facilities for active flight test work this project could not have been attempted.

TABLE OF CONTENTS

SUMMARY

This study was carried out in an effort to determine the longitudinal stability derivatives of a Ryan Navion airplane using dynamic flight testing methods. This was done by recording the transient response of the airplane to elevator forcing functions in the form of steps or pulses. Data reduction was carried out using the equations of motion method and the derivative method. Due to partial failure of the instrumentation the results from the equations of motion method were disappointing. More successful results were obtained using the derivative method in conjunction with the useful data acquired from the equation of motion method.

Concurrent with this report an investigation was carried out to find the stability derivatives of the same airplane from both theoretical considerations and from steady state flight testing. This investigation is described in Reference 7. An effort has been made to correlate the flight test results obtained from the dynamic and steady state methods and predictions made from theory. This correlation appears in Appendix B.

Reasonable values of C_{L_α} were obtained from dynamic testing which were consistent with speed, and position of center of gravity changes.

Dynamic testing also gave reasonable values for the damping derivatives which were consistent at the same speed, but which indicated an increase in the damping derivatives with increase in speed.

The proper changes in values for the stick fixed maneuver margin were found as the position of the center of gravity was changed, however a decrease in maneuver margin was found as speed was increased.

The elevator power was found with good consistency as the center of gravity was changed, but decreased in value as the speed was increased.

All values of C_{m_δ} were somewhat high as compared with theoretical values.

An attempt was made to explain the changes in C_{m_δ} and stick fixed maneuver margin that occurred with speed changes in terms of aircraft non-linearities.

LIST OF SYMBOLS

C_{L_o} = steady state lift coefficient.

$C_{m_\alpha} = \frac{\partial C_m}{\partial \alpha}$ partial derivative of the moment coefficient with respect to angle of attack.

$C_{m_{d\alpha}} = \frac{\partial C_m}{\partial d\alpha}$ partial derivative of the moment coefficient with respect to $d\alpha = \tau\dot{\alpha}$.

$C_{m_{d\theta}} = \frac{\partial C_m}{\partial d\theta}$ partial derivative of the moment coefficient with respect to $d\theta = \tau\dot{\theta}$.

$C_{m_\delta} = \frac{\partial C_m}{\partial \delta}$ elevator power = partial derivative of the moment coefficient with respect to elevator angle.

$C_{L_\alpha} = \frac{\partial C_L}{\partial \alpha}$ slope of the lift curve

C_m = $\frac{\text{(Pitching moment, ft. lbs.)}}{\frac{1}{2}\rho V^2 S \bar{C}}$

α = perturbation angle of attack, radians.

θ = perturbation angle of pitch (positive nose up) radians.

$d\theta = d\theta/dt/\tau = \tau\dot{\theta}$ radians.

$d^2\theta = \tau^2\ddot{\theta}$ radians.

n = perturbation normal acceleration (positive for push over maneuvers).

$\int n = \int n\, dt/\tau = \frac{1}{\tau}\int n\, dt$

δ = perturbation elevator angle, radians.

$\int \delta = \int \delta\, dt/\tau = \frac{1}{\tau}\int \delta\, dt$

F_s = stick force, lbs.

$d\epsilon/d\alpha$ = rate of change of downwash with angle of attack.

V = velocity, feet per second.

m = mass of the airplane, slugs.

$\mu = m/\rho S \bar{c}$

$\tau = m/\rho S V$ seconds.

I = moment of inertia of the airplane about the Y-axis, slug ft.^{2}

$h = 2 K_y^2/\mu \bar{c}^2$

$K_y = \sqrt{I/m}$, radius of gyration, feet.

$\bar{c}$ = mean aerodynamic chord, feet.

S = wing area, square feet.

ℓ = tail length, distance from the center of gravity to the aerodynamic center of the tail, feet.

S_w = 184.2 ft.^{2} = wing area.

S_t = 43 ft^2 = horizontal tail area.

S_e = 15.04 ft^2 = elevator area.

A_w = 6.04 = aspect ratio of wing

A_t = 3.98 = aspect ratio of horizontal tail.

b_w = 33.38 ft = wing span

b_t = 13.17 ft = tail span

$\bar{c}_w$ = 5.7 ft = mean aerodynamic chord of wing.

$\bar{c}_t$ = 3.34 ft = mean aerodynamic chord of horizontal tail.

ℓ = 15.04 ft = tail length, distance between center of gravity and aerodynamic center of the tail.

a.c. = .24 = position of wing aerodynamic center in %

i_w = 2° at root = incidence of wing
1° at tip

i_t = -3° = incidence of horizontal stabilizer.

Dihedral = 7.5°

INTRODUCTION

Dynamic testing of aircraft for stability parameters has received increased emphasis with the advent of guided missiles, sonic, and supersonic aircraft. Some of the major efforts in this field have been dynamic testing of a B-25 by Marshall E. Mullins at Edwards Air Force Base, (Ref. 4); the dynamic testing of an F-30A by R. C. Kidder at Cornell Aeronautical Laboratories, Inc. (Ref. 5); and guided missile testing by The Naval Air Missile Test Center, Pt. Mugu, California. In all previous cases no effort has been made to compare the results with those obtained by steady state flight test methods for the same aircraft. This report is part of a triple project on a Ryan Navion in which dynamic results are to be compared with theoretical and steady state results. The actual comparisons are included in Appendix B.

The dynamic testing with which this report is concerned consists of analysis of the transient response of the aircraft to an elevator forcing function. Using various forms of the equations of motion the stability parameters for the airplane were reduced from the data by the method of averages, least squares, and by the use of graphical plots.

THEORY AND ANALYSIS

The normal procedure in the determination of aircraft transient motions is to solve the differential equations which describe the aircraft motion. In doing this the constant coefficients in the equations of motion are estimated from theoretical considerations or measured by steady state test methods.

The problem dealt with in this report is the inverse of that stated above; ie., the determination of the coefficients in the equations of motion if the time history of the aircraft transient motions are known. The response history of the aircraft can be displayed as a function of frequency as well as time. In theory the response in either the time or frequency domain can be analyzed to determine the constant coefficients in the equations of motion. This report deals with the determination of the constant coefficients of the longitudinal equations of motion from transient responses displayed in the time domain.

Development of Equations:

Throughout this report it is assumed that the incremental changes in forward velocity are negligible. With this assumption the equations of motion as developed in Ref. 1 are:

$$\frac{C_{L_\alpha}}{2}\alpha + d\alpha - d\theta = 0 \tag{1}$$

$$C_{m_\alpha}\alpha + C_{m_{d_\alpha}}d\alpha + C_{m_{d\theta}}d\theta - h d^2\theta + C_{m_\delta}\delta = 0 \tag{2}$$

If elevator lift is considered important, its effect can be included in the lift equation since:

$$C_{L_\delta} = \frac{-C_{m_\delta}}{\ell/c} \tag{3}$$

Substitution in equation (1) yields:

$$\frac{C_{L_\alpha}}{2}\alpha' + d\alpha - d\theta - \frac{C_{m_\delta}}{2\,\ell/c}\delta = 0 \tag{4}$$

Solving equation (4) for $d\alpha$ and substitution in equation (2) yields:

$$\left(C_{m_\alpha} - \frac{C_{m_{d\alpha}} C_{L_\alpha}}{2}\right)\alpha + \left(C_{m_{d\alpha}} + C_{m_{d\theta}}\right)d\theta - h d\ddot{\theta} + C_{m_\delta}\left(1 + \frac{C_{m_{d\alpha}}}{2\,\ell/c}\right)\delta = 0 \tag{5}$$

Normal acceleration, n, and elevator angle, δ, may be substituted for α since:

$$\alpha = -\frac{C_L}{C_{L_\alpha}} n + \frac{C_{m_\delta}}{C_{L_\alpha}\,\ell/c}\delta \tag{6}$$

Substitution of this expression for α into equation (5) yields:

$$-C_L\left(\frac{C_{m_\alpha}}{C_{L_\alpha}} - \frac{C_{m_{d\alpha}}}{2}\right)n + \left(C_{m_{d\theta}} + C_{m_{d\alpha}}\right)d\theta + C_{m_\delta}\left(1 + \frac{C_{m_\alpha}}{C_{L_\alpha}\,\ell/c}\right)\delta - h d\ddot{\theta} = 0 \tag{7}$$

This equation if integrated once with respect to t/τ yields:

$$-C_L\left(\frac{C_{m_\alpha}}{C_{L_\alpha}} - \frac{C_{m_{d\alpha}}}{2}\right)\int n\, d\,t/\tau + \left(C_{m_{d\theta}} + C_{m_{d\alpha}}\right)\theta + C_{m_\delta}\left(1 + \frac{C_{m_\alpha}}{C_{L_\alpha}\, l/c}\right)\int \delta\, d\,t/\tau$$
$$- h\, d^2\theta = 0. \tag{8}$$

It is possible also to eliminate all variables except n, δ and their derivatives from equations (2) and (4). Solving equation (4) for $d\theta$ and $d^2\theta$ and substituting these into equation (2) yields:

$$\left(C_{m_\alpha} + \frac{C_{L_\alpha} C_{m_{d\theta}}}{2}\right)\alpha + \left(C_{m_{d\alpha}} + C_{m_{d\theta}} - \frac{h\, C_{L_\alpha}}{2}\right) d\alpha - h\, d^2\alpha$$
$$+ C_{m_\delta}\left(1 - \frac{C_{m_{d\theta}}}{2\, l/c}\right)\delta + \frac{h\, C_{m_\delta}}{2\, l/c}\, d\delta = 0 \tag{9}$$

Solving equation (6) for $d\alpha$, and $d^2\alpha$ in terms of n and δ yields:

$$d\alpha = \frac{-C_L}{C_{L_\alpha}}\, dn + \frac{C_{m_\delta}}{C_{L_\alpha}\, l/c}\, d\delta \tag{10}$$

$$d^2\alpha = \frac{-C_L}{C_{L_\alpha}}\, d^2n + \frac{C_{m_\delta}}{C_{L_\alpha}\, l/c}\, d^2\delta \tag{11}$$

Substituting equations (6), (10), and (11) into equation (9) yields:

$$d^2\eta + C_{m_\delta}\left(\frac{C_{m_\alpha}}{h\,\ell/c\,C_L} + \frac{C_{L_\alpha}}{h\,C_L}\right)\delta + \frac{C_{m_\delta}}{\ell/c\,h\,C_L}\left(C_{m_{d\theta}} + C_{m_{d\alpha}}\right)d\delta$$

$$- \frac{C_{m_\delta}}{\ell/c\,C_L}d^2\delta + \left(\frac{C_{L_\alpha}}{2} - \frac{C_{m_{d\theta}}}{h} - \frac{C_{m_{d\alpha}}}{h}\right)d\eta$$

$$- \left(\frac{C_{m_\alpha}}{h} + \frac{C_{m_{d\theta}}\,C_{L_\alpha}}{2h}\right)\eta = 0 \qquad (12)$$

Equation (12) if integrated once may be expressed as:

$$C_{L_\alpha}\left(\frac{C_{m_\alpha}}{C_{L_\alpha}} + \frac{C_{m_{d\theta}}}{2}\right)\int\eta - C_{m_\delta}\left(\frac{C_{L_\alpha}}{C_L} + \frac{C_{m_\alpha}}{C_L\,\ell/c}\right)\int\delta = v \qquad (13)$$

where

$$v = \left(\frac{C_{L_\alpha}h}{2} - C_{m_{d\alpha}} - C_{m_{d\theta}}\right)\eta - \frac{C_{m_\delta}h}{C_L\,\ell/c}d\delta + \frac{C_{m_\delta}}{C_L\,\ell/c}\left(C_{m_{d\alpha}} + C_{m_{d\theta}}\right)\delta + h\,d\eta \qquad (14)$$

Throughout the remainder of this report the following quantities are defined as:

$$A = -C_L\left(\frac{C_{m_\alpha}}{C_{L_\alpha}} - \frac{C_{m_{d\alpha}}}{2}\right) \tag{15}$$

$$B = C_{m_{d\theta}} + C_{m_{d\alpha}} \tag{16}$$

$$C = C_{m_\delta}\left(1 + \frac{C_{m_\alpha}}{C_{L_\alpha}\, \ell/c}\right) \tag{17}$$

$$L = C_{L_\alpha}\left(\frac{C_{m_\alpha}}{C_{L_\alpha}} + \frac{C_{m_{d\theta}}}{2}\right) \tag{18}$$

$$M = -C_{m_\delta}\left(\frac{C_{L_\alpha}}{C_L} + \frac{C_{m_\alpha}}{C_L\, \ell/c}\right) \tag{19}$$

Substituting equation (15) through (19) into equations (7), (8) and (13) yields:

$$An + Bd\theta + C\delta = hd^2\theta \tag{20}$$

$$A\int n + B\theta + C\int\delta = hd\theta \tag{21}$$

$$L\int n + M\int\delta = v \tag{22}$$

Equation (22) may be further rearranged as:

$$L\,\frac{\int n}{v} + M\,\frac{\int\delta}{v} = 1 \tag{23}$$

Solution of Equations:

In order to solve the equations of motion for values of the derivatives, one quantity must be known. In this case the known quantity was the airplanes moment of inertia about the Y axis. To determine the moment of inertia, the airplane was oscillated about the jack points as shown on Fig. 1.

If it is assumed that the airplane as suspended represents a second order system with zero damping, it is possible to determine the moment of inertia about the jack points, from the formula shown on Fig. 1. The moment of inertia was then transferred to the center of gravity. The position of the center of gravity was determined by using scales under each jack point and under the tail for two different inclinations of the airplane. With the moment of inertia about the center of gravity known it was possible to determine h about the center of gravity. By keeping an accurate record of weight added to and removed from the airplane h was determined for each run. The accurate determination of this quantity for each run is very important as small errors in h cause large errors in the solution for the constants in the equations of motion, equations (20), (21), or (23).

Examination of the equations of motion shows it would be most desirable to measure δ_e , α , $d\theta$, and $d^2\theta$ directly. Since an angular accelerometer was not available, direct measurement of $d^2\theta$ was impossible. Equation (6) shows the desirability for having normal acceleration data in order to determine C_{L_α} . For this reason, and realizing that there are certain inherent difficulties associated with the accurate determination of α, it was decided to use normal acceleration as one of the measured variables. In order to make the same instrumentation system available for use with steady state data and so that the elevator hinge moment equation might be considered in future studies, it was decided to include stick force as one of the measured variables. The resulting instrumentation yielded simultaneous values of α, n, δ_e , $d\theta$, and F_s. The actual circuits used are described in Appendix A.

Since h is a measured quantity, measurement of n, δ_e, $d\theta$, and $d^2\theta$ at three different values of time would permit the solution of equation (20).for A, B, and C. In like manner measurement of $\int n$, θ, $\int \delta_e$ and $d\theta$ at three values of time would permit the solution of equation (21) for A, B, and C. Knowledge of $\int n$ and $\int \delta_e$, and v for two values of time would permit the solution of equation (22) for L and M.

Methods of handling redundant data:

If the data were perfect, evaluation of the variables at only three instants of time would be sufficient to uniquely determine the coefficients of equations (20) and (21). With less than perfect data, however, some method must be used to determine the set of coefficients which most logically fit the data. The authors have used several methods of handling the redundancy arising from evaluation of the variables at many values of time. The first was a simple application of least squares assuming the error to be all in one variable: the second was a method of averages: the third was a graphical plotting method. This latter method is the most desirable since it gives a physical picture of the data scatter and the fairing process. The lack of physical feeling for the fairing process when least squares or averages are used to reduce the data is of great importance.

When the method of least squares was used the normal equations of equation (20) assuming all errors in $d^2\theta$ are:

$$A\Sigma n^2 + B\Sigma n\,d\theta + C\Sigma n\delta = h\Sigma n\,d^2\theta \qquad (24)$$

$$A\Sigma n\,d\theta + B\Sigma(d\theta)^2 + C\Sigma\delta\,d\theta = h\Sigma d\theta\,d^2\theta \qquad (25)$$

$$A\Sigma n\delta + B\Sigma\delta\,d\theta + C\Sigma\delta^2 = h\Sigma\delta\,d^2\theta \qquad (26)$$

In applying the method of least squares it was necessary to carry as many places as possible in combining the variables and solving the simultaneous equations. No justification is offered for the apparent inconsistency of carrying eight to ten significant figures in the summations of the various combinations of variables when the variables themselves cannot be taken from data sheets with more than three significant figures. It is merely stated as a finding that as many places as possible must be used in order to get reasonable answers using least squares procedures. It follows that least squares procedures should not be attempted without the use of an eight to ten place calculating machine. It is also to be noted as a corollary of the above that least squares procedures are very unforgiving of small errors in data transcription, summations, etc.

The method of averages consists of simply using the average values of n, $d\theta$, δ, and $d^2\theta$ taken from random groupings of the individual data. The best results were obtained by simply grouping the data into approximately even thirds. The first of the three simultaneous equations then would be made up of the summations of the variables over the first third of the time traces considered appropriate. This method consisted of dividing the data into three such groups. The simplicity and speed are such great advantages over even the simplest application of least squares that its applicability should be at least evaluated in any extensive data reduction problems.

Practical Considerations

Data for eight runs were reduced using any or several of the methods described above. The results were consistent for different methods applied to the same run but the only answer which seemed appropriate was

the value for B = $(C_{m_{d\theta}} + C_{m_{d\alpha}})$. The values of A and C were of improper magnitude and inconsistent from run to run. With this in mind the equations for the unknowns A, B, C in determinant form were examined.

$$A = \frac{h \begin{vmatrix} \sum_{9}^{12} d^2\theta & \Sigma d\theta & \Sigma \delta \\ \sum_{5}^{8} d^2\theta & \Sigma d\theta & \Sigma \delta \\ \sum_{1}^{4} d^2\theta & \Sigma d\theta & \Sigma \delta \end{vmatrix}}{\begin{vmatrix} \Sigma n & \Sigma d\theta & \Sigma \delta \\ \Sigma n & \Sigma d\theta & \Sigma \delta \\ \Sigma n & \Sigma d\theta & \Sigma \delta \end{vmatrix}} \qquad (27)$$

$$B = \frac{h \begin{vmatrix} \Sigma n & \Sigma d^2\theta & \Sigma \delta \\ \Sigma n & \Sigma d^2\theta & \Sigma \delta \\ \Sigma n & \Sigma d^2\theta & \Sigma \delta \end{vmatrix}}{\begin{vmatrix} \Sigma n & \Sigma d\theta & \Sigma \delta \\ \Sigma n & \Sigma d\theta & \Sigma \delta \\ \Sigma n & \Sigma d\theta & \Sigma \delta \end{vmatrix}} \qquad (28)$$

$$C = \frac{h \begin{vmatrix} \Sigma n & \Sigma d\theta & \Sigma d^2\theta \\ \Sigma n & \Sigma d\theta & \Sigma d^2\theta \\ \Sigma n & \Sigma d\theta & \Sigma d^2\theta \end{vmatrix}}{\begin{vmatrix} \Sigma n & \Sigma d\theta & \Sigma \delta \\ \Sigma n & \Sigma d\theta & \Sigma \delta \\ \Sigma n & \Sigma d\theta & \Sigma \delta \end{vmatrix}} \qquad (29)$$

Examination of equations (27), (28), and (29) shows that equation (28) is the only one where an error in the pitch rate gyro calibration would not affect the results.

An examination of the pitch rate gyro revealed that considerable friction had developed in the bearings and it was very doubtful if the gyro wheel was getting up to governing speed.

If it is assumed that the gyro maintains a constant speed during the 1.5 seconds during which data is being taken for any particular run, the reduced values of B will be correct. Values of A and C will of course be directly dependent on the gyro speed for that particular run.

Because of time limitations it was impossible to repair the gyro, recalibrate, and take new data. This necessitated re-examination of the equations of motion in order to eliminate pitch rate as an unknown. The method is very similar to that proposed in Ref. 2 and called the derivative method.

An examination of equation (14) shows that if $(C_{m_{d\alpha}} + C_{m_{d\theta}})$ and C_{L_α} are known, an estimation of C_{m_δ} will define the quantity v. Equation (23) is then recognized as that of a straight line where the variables are $\int n/v$ and $\int \delta/v$ and the intercepts with the coordinate axes determine values of L and M. At each instant of time it is only necessary to compute $\int n$, $\int \delta$, and v; make a plot of equation (13) on linear coordinates; and fair the best straight line through the points to determine the intercepts. These graphical plots were extremely enlightening. They indicated that L can be determined to much greater accuracy than can M. A blind application of least squares or averages could never indicate this

condition. Knowledge of this condition would be valuable for deciding in which variable to minimize the error for application of least squares.

It should also be noted that the answers are very insensitive to the estimated values used since the known value of $(C_{m_{d\alpha}} + C_{m_{d\theta}})$ makes up the major part of v.

In the process of data reduction it was attempted, with poor results, to use α data instead of n for solving the moment equation. The fifteen hundred series runs yielded very poor results. This was accounted for by the fact that an accurate in-flight calibration of the angle of attack indicator to account for vane position error effects was never attained for these runs. The nature of the difficulty is described in Appendix A.

The α data was used in equation (6) to obtain values of C_{L_α}. The use of α data necessitates taking into account the effect of up wash and the effect of pitching velocity. The effect of up wash is determined from steady flight calibration of the angle of attack indicator. The effect of pitching velocity is determined by measuring the distance of the vane ahead of the center of gravity and computing the velocity component at the vane due to pitch rate. Another effect that it was not possible to account for quantitatively was the effect of acceleration in pitch. Due to flexibility of the boom angular acceleration of the airplane caused bending of the boom in such a manner that individual values of the C_{L_α} determined at each instant of time yielded a plot as shown below. Better stiffening of the boom should eliminate this source of error.

As the dynamic response of the angle of attack vane was not deter-

mined, any natural dynamic response of the vane consisted of an error in the α data of undetermined magnitude.

For the above reasons α data was used only to determine C_{L_α} from the sixteen hundred runs.

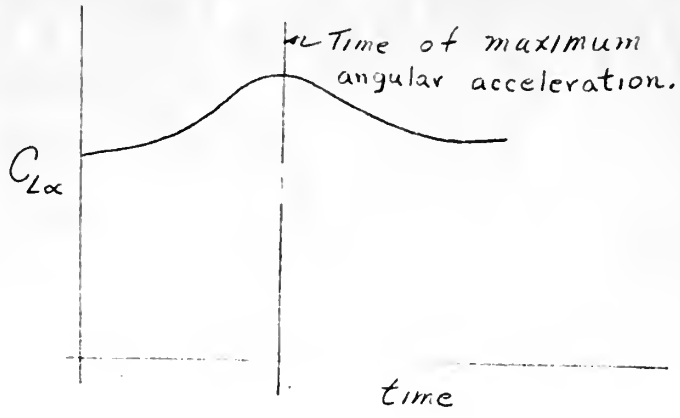

The solution of the equations of motion by any of the techniques used does not allow solution for unique values of the derivatives $C_{m_{\dot{\alpha}}}$, C_{m_α}, C_{m_δ}, and $C_{m_{\dot{\theta}}}$. In order that the results may contain approximate values for the above derivatives it was assumed that $C_{m_{\dot{\alpha}}} = \frac{d\epsilon}{d\alpha} C_{m_{\dot{\theta}}}$ and $\frac{d\epsilon}{d\alpha} = .5$. It is important to realize that without the above assumption dynamic flight test procedures as described herein do not yield unique answers for the individual derivatives.

PROCEDURE

The procedure followed in this report may be considered in the following parts: 1. Instrumentation, 2. Calibration, 3. Flight test, 4. Data reduction.

1. Instrumentation

The design, construction, and installation of the instruments used in this report took approximately four months. The circuits actually used as well as the design criteria may be found in Appendix I. The reasons for the choice of variables to be measured may be found in the Theory and Analysis section of this report.

2. Calibration

The calibration curves for each circuit used may also be found in Appendix A. A brief explanation of inherent difficulties in measuring certain variables may be found in the Theory and Analysis section of this report. Calibration was, of course, carried out continuously as the flight test progressed to insure that the calibration curves remained applicable. The one exception to the above statement was the calibration of the pitch rate gyro. It was calibrated in the final stages of instrument installation at the Naval Air Test Center, Patuxent River, Maryland, and no further calibrations were performed. The difficulties encountered in the early stages of data reduction emphasized the desirability of continuous calibration checking.

3. Flight test

The flight procedure for transient dynamic testing is extremely

simple and represents the greatest advantage of dynamic testing over steady state testing methods. Smooth air is essential in order that a good steady state flight condition may be attained. After attainment of a good steady state condition, the steady state is disturbed in some predetermined manner. Pulse type elevator forcing functions were applied by simply moving the yoke a predetermined amount, holding it in the new position for approximately one second, and then returning it to the original position. The resulting pulses were poor approximations to an analytical pulse. However, in an equations of motion technique this was not important. The best method found for applying a step elevator input consisted of holding the stick against the force caused by a preset value of trim tab and then simply letting go of the stick. The elevator is so heavily damped that the resulting elevator motion was very nearly a step.

All data was taken at 19.5 inches manifold pressure and about 1850 engine revolutions per minute. Low engine speeds were required to reduce angle of attack boom resonance. Variations in speed were obtained by varying the rate of descent. Data was taken for two center of gravity positions and two speeds using both pulse and step elevator forcing functions.

4. Data reduction

The various methods of data reduction are described in the Theory and Analysis section of this report.

SAMPLE CALCULATIONS

A sample of each type of calculation is carried out in this section to further clarify the procedure used. The calculations are carried out on run #1640. The values of the variables taken from run #1640 may be found in Table II. Table I contains the various constants required in the calculations and the calibration factors taken from the calibration curves.

Equation (21) is

$$A\int n + B\theta + C\int \delta = h\,d\theta$$

The values for $\int n$, θ , $\int \delta$ and $d\theta$ may be obtained for each point indicated in Table II since:

$$\int n\, d{}^{t}/_{\tau} = \frac{1}{\tau}\int n\,dt = \frac{C_n}{\tau}\int n\,dt \text{ (inch seconds)}$$

where C_n = calibration factor for n in g's/in.

$$\int \delta\, d{}^{t}/_{\tau} = \frac{C_\delta}{\tau}\int \delta\,dt \text{ (inch seconds)}$$

$$\int d\theta\, d{}^{t}/_{\tau} = \theta = C_{d\theta}\int \dot{\theta}\,dt \text{ (inch seconds)}$$

$$d\theta = \frac{d\theta}{d{}^{t}/_{\tau}} = \tau\dot{\theta} = \tau\, C_{d\theta}\,\dot{\theta} \text{ (inches)}$$

With values of the variables at each point three simultaneous equations may be obtained as follows where the summations are over the various points of time:

$$A\sum_{1}^{4}\int n\,dt_2 + B\sum_{1}^{4}\theta + C\sum_{1}^{4}\int\delta\,dt_2 = h\sum_{1}^{4}d\theta$$

$$A\sum_{5}^{8}\int n\,dt_2 + B\sum_{5}^{8}\theta + C\sum_{5}^{8}\int\delta\,dt_2 = h\sum_{5}^{8}d\theta$$

$$A\sum_{9}^{12}\int n\,dt_2 + B\sum_{9}^{12}\theta + C\sum_{9}^{12}\int\delta\,dt_2 = h\sum_{9}^{12}d\theta$$

Actual calculations yielded the following simultaneous equations:

$$-.000091\,A + .017371\,B - .020173\,C = .010376$$

$$-.198996\,A + .110355\,B - .074817\,C = .020030$$

$$-.601369\,A + .204940\,B - .125027\,C = .014376$$

Solution of these equations simultaneously for B gives B = - .141841.

It is clear that equation (7) as it stands could be solved using values of δ, n, $d\theta$, and $d^2\theta$. These variables in inches and seconds units are also included in Table II.

If equation (6) is rearranged it is possible to solve for C_{L_α}.

$$C_{L_\alpha} = \frac{-C_L n + \frac{C_{m_\delta}\,\delta}{l/c}}{\alpha}$$

Values of n, δ, and α may be obtained from Table II using the calibration factors of Table I. The value of α so obtained should be further corrected for the error introduced in the vane indicator by pitching velocity.

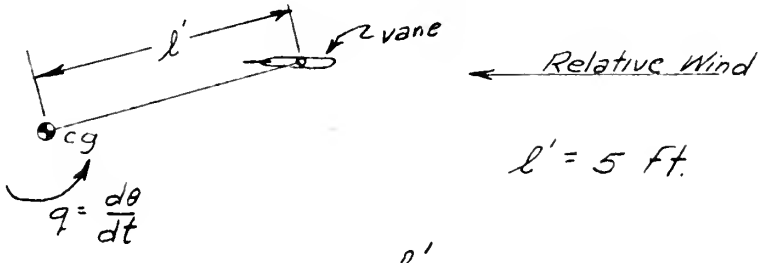

$$\Delta\alpha = \frac{q l'}{V}$$

where V is true velocity in ft/sec.

It is necessary to estimate C_{m_δ} . C_{m_δ} was estimated theoretically to be -1.3. An incorrect value of C_{m_δ} will of course be reflected in an incorrect value of C_{L_α} but the percentage error in C_{L_α} will be much less than the percentage error in C_{m_δ} . Using all points of Table II the following equation was obtained:

$$C_{L_\alpha} = \frac{-C_L \sum_1^{12} n + \frac{C_{m_\delta}}{\ell/c} \sum_1^{12} \delta}{\sum_1^{12} \alpha}$$

$$C_{L_\alpha} = \frac{-(.744)(-3.4479) + \frac{(-1.3)(-.645)}{2.64}}{.537}$$

$$C_{L_\alpha} = \frac{2.66 + .16}{.537} = 5.06$$

For this particular case an increase in C_{m_δ} of 50% gives an increase of 12% in C_{L_α}.

The terms on the right hand side of equation (13) have been estimated as shown at the end of this section for runs #1522, 1523, 1640, and 1652. These estimated quantities have been determined using values of $(C_{m_{d\alpha}} + C_{m_{d\theta}})$ determined by equations of motion method and as rationalized in Fig. 2. An average value of C_{L_α} and the theoretical value of $C_{m_\delta} = -1.3$ have also been used in these estimations. Tables III, IV, V, and VI contain

the calculations for v and the variables $\delta n/\sigma$ and $\delta\theta/\sigma$. These variables are plotted and the values of L and M determined on Figs. 3 and 4.

ESTIMATES FOR COMPONENTS IN $\dot{\alpha}$ OF DERIVATIVE METHOD.

RUN # 1522

$$-\left[C_{m_{d\alpha}} + C_{m_{d\theta}} - \frac{C_{L_\alpha} h}{2}\right] = .275 + \frac{(5)(.0609)}{.2} = +.427$$

$$-\frac{C_{m_\delta} h}{C_L \; c/c} = -\frac{(1.3)(.0609)}{(.461)(2.64)} = +.0650$$

$$\frac{C_{m_{\bar{\delta}}}}{C_L \; c/c}\left(C_{m_{d\alpha}} + C_{m_{d\theta}}\right) = \frac{(1.3)(-.275)}{(.461)(2.64)} = +.293$$

RUN # 1528

$$-\left[C_{m_{d\alpha}} + C_{m_{d\theta}} - \frac{C_{L_\alpha} h}{2}\right] = .205 + \frac{(5)(.06)}{2} = .355$$

$$-\frac{h\, C_{m_\delta}}{C_L \; c/c} = -\frac{(.06)(-1.3)}{(.686)(2.64)} = +.0431$$

$$\frac{C_{m_\delta}}{C_L \; c/c}\left(C_{m_{d\alpha}} + C_{m_{d\theta}}\right) = \frac{(-1.3)(-.205)}{(.686)(2.64)} = +.147$$

RUN # 1640

$$-\left[C_{m_{d\alpha}} + C_{m_{d\theta}} - \frac{C_{L_\alpha} h}{2}\right] = .205 + \frac{(5)(.0441)}{2} = .3164$$

$$-\frac{C_{m_\delta} h}{C_L \; c/c} = \frac{-(-1.3)(.0441)}{(.744)(2.64)} = .0292$$

$$\frac{C_{m_\delta}}{C_L \; c/c}\left(C_{m_{d\alpha}} + C_{m_{d\theta}}\right) = \frac{(-1.3)(.205)}{(.744)(2.64)} = .136$$

RUN #1652

$$-\left[C'_{m_{d\alpha}} + C'_{m_{d\theta}} - \frac{C'_{L_\alpha} h}{2}\right] = .275 + \frac{(5)(.0467)}{2} = .3918$$

$$-\frac{h\, C'_{m_\delta}}{C'_L\ \ell/c} = -\frac{(.0467)(-1.3)}{(.473)(2.64)} = .0486$$

$$\frac{C'_{m_\delta}}{C'_L\ \ell/c}\left[C'_{m_{d\alpha}} + C'_{m_{d\theta}}\right] = \frac{(-1.3)(-.275)}{(.473)(2.64)} = .286$$

RESULTS

The following is a tabulation of the most important results.

FLIGHT CONDITION	RUN	$Cm_{d\theta} + Cm_{d\alpha}$	$C_{L\alpha}$	$Cm_{d\alpha}$ *	$Cm_{d\theta}$ *	$\frac{Cm_q}{C_{L\alpha}} + \frac{Cm_{d\theta}}{2}$	$Cm_{\dot{\alpha}}$ *	Cm_δ
cg = 30.2% 90 mph	1524 n	-.200		-.067	-.134			
	1524 n	-.223		-.074	-.148			
	1528 n	-.193		-.064	-.128	-.287	-1.09	-2.30*
	1528 n	-.194		-.065	-.130			
cg 23.8% 90 mph	1640 n	-.145		-.048	-.096	-.346	-1.39	-2.21
	1645 n	-.220		-.073	-.146			
	1645 α		4.96					
	1640 α		5.06					
cg 30.2% 110 mph	1520 n	-.285		-.095	-.190			
	1522 n	-.268		-.089	-.178	-.222	-.665	-1.72 *
cg 23.8% 110 mph	1648 n	-.285		-.095	-.190			
	1648 α		4.98					
	1652 n	-.140		-.047	-.094	-.272	-.900	-1.84
	1652 α		4.98					

* values corrected for δ_e calibration data.

** $\frac{d\epsilon}{d\alpha} = 0.5$ assumed.

RESULTS

The values of C_{L_α} were consistent with theoretical considerations and no trends were indicated as speed and center of gravity position were changed.

The damping derivatives were found with good consistency at the same speed but an increase in damping derivatives ($C_{m_{d\alpha}} + C_{m_{d\theta}}$) was found with increase in speed.

The values of stick fixed maneuver margin $\left[\frac{C_{m_\alpha}}{C_{L_\alpha}} + \frac{C_{m_{d\theta}}}{2} \right]$ indicated a change of the proper amount when center of gravity position was changed at constant speed. However, a decrease in stick fixed maneuver margin was found as speed was increased. The stick fixed maneuver point for 90 mph was 58%, for 110 mph it was 52%.

The value of C_{m_δ} was found with some consistency at each speed, but a decrease was indicated in C_{m_δ} as speed was increased. The values of C_{m_δ} were somewhat high in comparison with theoretical values.

The only immediately apparent enigmas in the results then seemed to arise as a result of speed changes. This would lead one to suspect an error in some or all of the constants used in data reduction which were functions of speed. These constants are γ , and C_L. The values of γ and C_L used were very carefully examined and no errors could be found.

During the in-flight calibration of the angle of attack indicator a condition was found which might explain some of these changes with speed. A sharp increase in up wash at the wing tip was noted as speed was decreased below 85 mph indicated. The test aircraft was equipped with a spoiler near the wing root. The possibility existed, then, that non-linearities in flow

and lift were occurring during pull ups from the 90 mph steady state.

If non-linearities in the flow did exist, they would be reflected in low values of normal acceleration. Further the actual error in the normal acceleration would become greater with time. The recorded values of normal acceleration would be less by a progressively larger amount than that which would have been recorded sans non-linearities. The recorded values of $\int n$ would have been less but not by as large a percentage as normal acceleration itself. The error in dn was not as apparent as that for n and $\int n$.

The equation from which C_{m_δ} and stick fixed maneuver margin were obtained was:

$$L \frac{\int n}{v} + M \frac{\int n}{v} = 1$$

The quantity v as determined in Tables III, IV, V, and VI was predominantly made up of n, particularly after the first few tenths of a second. The non-linearities discussed then, if present, would have tended to make $\frac{\int n}{v}$ and $\frac{\int \delta}{v}$ too large, the error increasing with time. Since $\frac{\int n}{v}$ was a larger quantity than $\frac{\int \delta}{v}$ these errors would tend to decrease the slope of the lines faired into the data in Figs. 3 and 4. This could have given the increased apparent stability found at lower speeds. Also since the points at later times were used predominantly in fairing Figs. 3 and 4, the increased value of C_{m_δ} at 90 mph could also be caused by these non-linearities.

An attempt to evaluate the effects of non-linearities on the values of the damping derivatives as determined by equations of motion method lead

to no definite conclusions. It is possible that some of the apparent increase in damping derivatives with speed may have been caused by low values of normal acceleration at the lower speed. The increase in damping derivatives with speed indicated an increase in tail efficiency. The test procedure required as low an RPM as possible to reduce the angle of attack boom resonance. Power used was 19.5 inches, full low RPM at both speeds. This required an increase in rate of descent with increase in speed. This does not appear consistent with the increase in tail efficiency unless the tail was operating in a particularly unfortunate position with respect to wing wake at the lower speed.

CONCLUSIONS AND RECOMMENDATIONS

Dynamic flight testing is in general a perfectly feasible method of accurately determining the stability derivatives of an airplane. Certain basic requirements for obtaining good results are as follows:

1. Inclusion of pitch rate as one of the measured variables.

2. Weight, moment of inertia, and airspeed must be known very accurately.

3. Instrumentation must be very accurate without unknown instrument dynamic characteristics.

Dynamic testing has the following advantages and disadvantages.

Advantages:

1. Simplicity of flight procedure.

2. Short duration of in flight testing.

3. Non-linear effects may be included in the equations of motion.

4. Values of the derivatives obtained are the ones the airplane feels in response to transient maneuvers. They are the values for velocity equal a constant.

5. Close correlation exists between frequency response determined from dynamic testing and auto pilot design requirements.

Disadvantages:

1. Instrumentation is generally very expensive.

2. Data reduction is long, tedious, and subject to error.

3. Some of the results can not be compared to static flight test results which are for $C_L V^2$ equal a constant.

In recommending that the work be continued the most important

improvements in the methods used are listed below.

1. Further efforts should be made to obtain accurate pitch rate data.

2. A pendulum or turntable should be constructed for calibration of the rate gyro and accelerometer.

3. An angular accelerometer would permit the measurement of $d^2\theta$ directly.

4. Angle of attach data would be improved by boom stiffening, and dynamic calibration of the vane.

5. A frequency analysis of the airplane response might yield interesting results.

REFERENCES

1. Perkins, C.D., and Hage, R.E. Airplane Performance Stability and Control. John Wiley and Sons, New York, N. Y.

2. Greenberg, Harry. A Survey of Methods for Determining Stability Parameters of an Airplane from Dynamic Flight Measurements. NACA TN 2340.

3. Shinbrot, Marvin. A Least Squares Curve Fitting Method With Applications to the Calculation of Stability Coefficients From Transient Response Data. NACA TN 2341.

4. Mullens, Marshall E. Longitudinal Frequency Response Characteristics of a B-25J Aircraft as Obtained by the Transient Method. Air Force Technical Report No. AFFTC 52-5.

5. Kidder, R.C. Dynamic Longitudinal Stability Flight Tests of an F-80A Airplane by the Forced Oscillation and Step Function Response Methods Including Measured Horizontal Tail Loads. Cornell Aeronautical Laboratory Report No. T.B.-495-F11 dated 10 February 1950.

6. Schumacher, L.E. A Method for Evaluating Aircraft Stability Parameters from Flight Test Data. Air Force Technical Report No. WADC-TR-52-71.

7. Schuld, E.P. and Reinhart, L.J., Determination of the Longitudinal Stability Parameters by Steady State Flight Testing and Theoretical Calculations for the Ryan Navion. Princeton University Aeronautical Engineering Laboratory Report No. 232.

APPENDIX A

Description of Test Equipment

The test airplane was a standard Ryan Navion instrumented to record time histories of elevator angle, angle of attack, stick force, pitch rate and normal acceleration. These variables were recorded with a Consolidated Engineering Corporation type 5-116-P3-14 recording oscillograph. A wiring diagram for the instrumentation system used is shown in Fig. 5. Schematic diagrams showing the operation of the individual circuits appear as Figs. 6 and 7.

Certain basic considerations were common to the design and operation of all of the circuits. These were:

(a) To make the equivalent resistance of each circuit be 350 ohms as seen from the oscillograph leads, in order to meet the manufacturer's recommendation for 62% of critical damping for optimum galvanometer response.

(b) To operate the sensitivity adjustment of each circuit at about 50% attenuation.

(c) To use as small balancing resistors as possible in order to maintain linearity of the output, and at the same time keep the resistors large enough to limit the current drawn from the battery.

(d) To obtain maximum galvanometer deflection for the range of variables measured at each flight condition. The galvanometer deflection was one inch per 12.4 μ amps of current.

Power for the instruments was obtained from a 45 volt dry cell battery with a center tap. Voltage from this battery to the bus lines was regulated to 20 volts for all tests using a variable resistor and voltmeter.

Elevator Angle and Angle of Attack Circuits. The δ_e and α circuits are shown schematically in Fig. 7. The potentiometers used to sense the angular motions were 12,500 ohm, Micro-Max precision potentiometers with outputs guaranteed to be linear within one per cent. The motion of the α vane and the elevator was transmitted to the potentiometer shafts in a one to one ratio. The 2500 ohm balancing potentiometer is used to adjust the circuit output to zero at various elevator or α-vane positions. The additional 5000 ohm resistors in series with the balancing potentiometer were required to limit the current drawn from the dry cell. The 1500 ohm load resistor was required to adjust the current to the galvanometer to the desired magnitude. Sensitivity adjustment was achieved through a 500 ohm impedance pad. The 1000 ohm variable shunt resistor was placed in parallel with the circuit to make the galvanometer external damping resistance be 350 ohms as required.

The calibration of the elevator angle circuit is shown in Figs. 8 and 9. These calibrations were made using a propeller protractor mounted on the elevator to measure $\Delta \delta_e$'s . Fine adjustments of the elevator position were made by moving the elevator with a hydraulic jack under the trailing edge.

Calibration of the angle of attack circuit was made in flight using the propeller protractor to measure $\Delta \alpha$'s . Calibrations were also made on the ground using a specially made fitting on the boom to measure the angle between the vane position and the boom centerline. These calibrations are shown in Figs. 10 and 11, and illustrate the difference in calibration under flight conditions caused by airloads on the vane and boom. Due to

an oscillograph breakdown it was impossible to get an in-flight calibration for the 1500 series runs before the sensitivity and zero balance settings were changed. Therefore the in-flight calibration for the 1500 series runs was made using the difference between ground and flight calibrations for the 1600 series runs and extrapolating for a correction to be added to the 1500 series ground calibration.

Stick Force, Pitch Rate and Normal Acceleration Circuits. The operation of the F_s, $\dot{\theta}$, and n circuits are similar and are shown schematically in Fig. 6. The strain gauge bridge circuits used to measure these variables will be described individually later. The 5000 or 50,000 ohm balancing potentiometer in each circuit gave a zero output adjustment to the circuit over a wide range of values of F_s, $\dot{\theta}$, and n. The 5000 or 50,000 ohm resistors in series with the balancing potentiometers were necessary to provide a current limit to protect the galvanometer in case the circuit should inadvertently be turned on with the sensitivity adjustment full open and the balancing potentiometer turned against the stops in either direction. The sensitivity adjustment and damping resistors are the same as described for the α and δ_e circuits.

The accelerometer used in the n circuit was a model F-1.5-880 accelerometer manufactured by the Statham Laboratories, Incorporated. The manufacturer's specifications required an 18 volt input to the accelerometer which was obtained with a 100 ohm variable resistor in series with the circuit leads to the power supply. The accelerometer had a range of $\pm$1.5 g's. The circuit was calibrated between zero and one g and assumed to be linear to 1.5 g. The calibration curve is shown in Fig. 12. The noise level in

the n circuit was extremely sensitive to airplane vibrations, particularly to engine rpm. In order to minimize this the π-section filter shown in Fig. 6 was used to filter out vibrations above 12 cycles per second.

The stick force bridge was made up of SR-4 strain gauges cemented to the spokes of a specially constructed force wheel which replaced the standard pilots wheel in the airplane. Calibration of the stick force circuit is shown in Fig. 13.

The pitch rate circuit bridge was made up of SR-4 strain gauges mounted on a leaf spring which restrained the precession of a gyroscope when the gyroscope was subjected to an angular velocity. The SR-4 strain gauge bridge requires a 15 volt input which was obtained by using a 100 ohm variable resistor in series with the circuit leads to the power supply. The pitch rate gyro was calibrated on a calibrating pendulum at the Naval Air Test Center, Patuxent River, Md., and subsequent recalibrations were not feasible. This calibration established the linearity of the circuit, and is shown in Fig. 14. This linearity extended through six points not appearing within the range of Fig. 14. A 250,000 ohm $\pm$0.1% and a 50,000 ohm $\pm$0.1% precision resistor was placed in parallel with one side of the bridge as shown in Figs. 5 and 6. At the time of the original pendulum calibration the bridge unbalance caused by these calibration resistors was noted to give a circuit output equivalent to particular values of pitch rate. Then with the instrument installed in the airplane a calibration could be made for each test flight. This was done by momentarily closing a calibration resistor switch with the aircraft in steady flight. A galvanometer deflection was thus obtained for a known value of pitch rate. This point

along with the point of zero deflection for zero pitch rate was then used to establish a calibration curve for the flight.

The electric motor in the gyroscope was powered from a 24 volt storage battery. It was discovered during the data reduction that the gyro motor had had a progressive bearing failure, and that $\dot{\theta}$ values were unreliable. This failure could have been discovered had a calibrating pendulum been available for calibration after each test flight.

APPENDIX A

The following is a tabulation of the results from Princeton Reports No. 231 and 232. Report No. 232 consists of the determination of longitudinal stability parameters, for a standard Ryan Navion, using theoretical calculations and steady state flight test techniques. Report No. 231 consists of determining as many as possible of these same parameters for the same airplane using dynamic flight testing techniques.

Clean - Power On

Parameter	Theoretical	Steady State	Dynamic
C_{L_α}		0.100	0.088
C_{m_δ}	-0.022	-0.023	-0.031
N_o	0.380	0.370	0.440
N_o'	0.420	0.440	
N_m	0.46	0.45	0.52
N_m'	0.53	0.59	
C_{m_α} (based on N_o)	-0.37	-0.39	
C_{m_α} (based on N_m)	-0.75		-0.67
$C_{m_{d\theta}}$	-0.17	-0.12	-0.18
$C_{m_{d\alpha}}$	-0.08	-0.06	-0.09

Clean - Power Off

Parameter	Theoretical	Steady State
C_{L_α}	.084	.090
C_{m_δ}	-.020	-.022
$C_{m_{d\alpha}}$	-.073	-.068
$C_{m_{d\theta}}$	-.15	-.13
N_o	.39	.39
N_o'	.42	.44
N_m	.46	.47
N_m'	.52	.51

Landing - Power On

Parameter	Theoretical	Steady State
C_{m_δ}	-.028	-.029
N_o	.39	.38
N_o'	.41	.43

Landing - Power Off

Parameter	Theoretical	Steady State
C_{m_δ}	-.020	-.024
N_o	.48	.41
N_o'	.50	.50

Examination of the tables above shows the following:

1. Values of C_{L_α} determined by the different methods were all within 12%.

2. Theoretical and steady state values of C_{m_δ} agree very closely while the value of C_{m_δ} from dynamic testing seems to be about 30% high. Some of this could be accounted for by the fact that non-linearities in the elevator angle potentiometer used for dynamic work caused a possibility of 10-15% error in idividual values of the elevator angle. However, it is improbable that the slope of the elevator angle calibration curve could be more than 10% off. In steady state testing, power for level flight was used. In the dynamic testing, less power was used in order to keep the engine RPM low to avoid angle of attack boom resonance. The 110 MPH air speed was attained by establishing a steady rate of descent.

3. The values of the stick fixed maneuver point $N_{m_{V=K}}$ again agree between theoretical and steady state values while the value from dynamic testing seems to be 17% high. The difference seems excessive since it represents a 47% descrepancy in the maneuver margin. The graphical plots of Figs. 3 and 4 of Report No. 231 indicate the difficulty of obtaining from dynamic data the intercept which determins the maneuver margin. Even though the intercept is defined by lines crossing at a small angle this can not account for the 47% discrepancy. Dynamic work was adversely hampered by failure of the rate gyro and continual investigation with accurate

rate gyro measurements may yield better results. The effect of carrying the lower power for the dynamic testing is also apparent when the power-off maneuver margin from steady state results is considered. If the values from dynamic testing are compared with the power-off values of steady state results the discrepancy is 27% indicating that the effect of carrying the lower power in dynamic testing may be very large.

The value of C_{m_α} obtained from steady state testing is much lower than that from dynamic testing for the same reasons causing the discrepancy in the maneuver margin. The difference in C_{m_α} is further accentuated by the small value of the damping derivatives obtained from steady state testing. The theoretical value of C_{m_α} determined from the stick fixed neutral point agrees with the value of C_{m_α} from steady state testing and the theoretical value of C_{m_α} determined from stick fixed maneuver point agrees fairly well with the value of C_{m_α} determined from dynamic tests. This shows that dynamic test results are very closely related to maneuvering stability while the steady state results are more nearly related to static stability.

The values of the damping derivatives $C_{m_{d\theta}}$ and $C_{m_{d\alpha}}$ obtained from theory and dynamic testing agree closely while those obtained from steady state testing are too low. This can be primarily accounted for by the fact that the damping derivatives are very difficult to extract from the steady state test data and are presumed to be in error.

4. The greatest variance between the theoretical and steady state flight test results, with the exception of parameters previously discussed, was found to be in the stick free maneuver point for the power-on, clean condition, and in the stick fixed neutral point for the power-off, landing condition .

It is believed that the discrepancy in the stick free maneuver point may be attributed to the fact that at low normal accelerations the stick force required is low and erroneous indications of stick force are possible because of the friction in the control column and elevator system. Data reduction and analysis indicated no change in maneuvering point between normal accelerations of 1.0 to 1.3. However, if an interpolation is made between the stick free maneuver point for normal accelerations of 1.0 to 1.5, a value of maneuver point of approximately 55% mean aerodynamic chord is obtained which corresponds quite closely with the 53% mean aerodynamic chord obtained from theoretical considerations.

The stick fixed neutral point for the power-off, landing condition which was obtained from steady state tests corresponds to the trends indicated in the other power conditions and configurations. However, the theoretical analysis indicated considerably more stability. Assignment of the error involved can not be done with any degree of accuracy; however, it is believed the major portion of the difference can be accounted for in the evaluation of the factor $\left(1-\frac{d\epsilon}{d\alpha}-\frac{d\epsilon_p}{d\alpha}\right)$ in the theoretical analysis.

TABLE I

TABLE OF FLIGHT TEST CONDITIONS

RUN	PRESSURE ALTITUDE feet	TEMP. °C	ρ slugs/ft^3	$\sqrt{\sigma}$	TRUE AIRSPEED ft/sec	WEIGHT OF A/C lbs	C_L	X_{cg} % mac	MASS OF A/C slugs	τ	μ	k_y^2	h
1520	5300	8.5	.002000	.9170	179	2733	.462	30.2	85.0	1.290	40.4	38.4	.0585
1522	4300	10	.002070	.9330	176	2721	.461	"	84.7	1.262	38.9	38.5	.0609
1524	5600	8	.001984	.9135	145.3	2708	.693	"	84.2	1.585	40.4	38.7	.0589
1528	5600	8	.001984	.9135	145.3	2683	.686	"	83.5	1.570	40.1	39.1	.0600
1640	7250	7	.001869	.8868	149.7	2874	.744	23.8	89.4	1.735	45.5	32.6	.0441
1645	7400	7	.001861	.8846	150	2858	.740	"	88.9	1.728	45.5	32.8	.0443
1648	7100	7	.001879	.8888	184.7	2849	.483	"	88.6	1.386	44.9	32.9	.0451
1652	6600	6	.001924	.8994	182.7	2836	.473	"	88.1	1.361	43.6	33.1	.0467

CALIBRATION FACTORS USED IN DATA REDUCTION

RUN	δ rad/inch osc. defl.	n g's/inch defl.	α rad/inch defl.	$\dot{\theta}$* rad/sec / inch defl.
1500 SERIES	.0637	.270	.0925	.0834*
1600 SERIES	.0558	.270	.0427	.0803*

*Unreliable. See description of test equipment section of report.

TABLE II

RUN # 1640

POINT	θ	$\dot{\theta}$	$\ddot{\theta}$	θ @ 1.5 sec	$\dot{\theta}$ @ 1.5 sec	θ @ 1.5 sec	θ	$\dot{\theta}$
1	-.36	+.06	-.06	+.045	-3.53	+.45	+.56	-.0115	+.00332
2	-1.05	+.11	0	+.300	-3.53	-.56	+1.52	-.0835	+.01382
3	-1.17	-.15	+.11	+.600	+.325	-1.57	+1.08	-.2030	+.01212
4	-1.11	-.51	+.38	+.765	+.240	-1.82	+.52	-.3170	-.0219
5	-1.07	-.88	+.66	+.835	+.210	-1.59	+.2	-.4255	-.0929
6	-1.04	-1.18	+.96	+.860	+.170	-1.13	0	-.5305	-.1974
7	-1.01	-1.45	+1.28	+.840	+.100	-1.105	-.17	-.6325	-.3299
8	-.99	-1.64	+1.53	+.785	+.085	-.720	-.32	-.7325	-.4839
9	-.97	-1.74	+1.72	+.720	+.085	-.405	-.38	-.8301	-.6544
10	-.95	-1.8	+1.82	+.630	+.060	-.155	-.43	-.9261	-.8324
11	-.93	-1.82	+1.87	+.550	+.075	+.1	-.42	-1.0211	-1.0139
12	-.93	-1.77	+1.86	+.470	+.070	+.31	-.34	-1.1146	-1.1934

POINT	$\int\theta$ IN-SEC	POINT	$\int\dot{\theta}$ IN-SEC	POINT	$\int\theta$ IN-SEC
1	+.00113	6	+.24393	11	+.66343
2	+.01713	7	+.37943	12	+.71443
3	+.06313	8	+.46093		
4	+.13243	9	+.53643		
5	+.21393	10	+.60343		

RUN # 1522

POINT	.427 n	.065 dδ	.293 δ	.0609 dn	v	∫n	∫δ	∫n/v	∫δ/v
2	+.0017	-.00397	-.01083	-.0311	-.0442	+.000774	-.00229	-.0175	+.0518
3	-.021	+.00016	-.01100	-.0483	-.08014	-.00094	-.00512	+.01235	+.063
4	-.0522	+.00041	-.01033	-.0596	-.12222	-.00738	-.00813	+.0604	+.0665
5	-.0874	+.00041	-.01064	-.0646	-.16223	-.01987	-.01094	+.1225	+.0674
6	-.1191	+.00041	-.01035	-.0501	-.17914	-.03864	-.01373	+.2160	+.0766
7	-.143	+.00041	-.01018	-.036	-.18377	-.06257	-.01645	+.3320	+.087
8	-.1605	+.00041	-.00998	-.0282	-.17289	-.09011	-.01912	+.5210	+.1105
9	-.1748	+.00041	-.0098	-.0236	-.18655	-.12054	-.02174	+.646	+.1165
10	-.1860	+.00041	-.0097	-.0149	-.21019	-.15334	-.02430	+.726	+.1153
11	-.193	+.00041	-.00951	-.0108	-.21290	-.18769	-.02685	+.880	+.126
12	-.198	+.00041	-.00934	-.0070	-.21393	-.22317	-.02932	+1.043	+.137
13	-.200	+.00041	-.00915	-.0010	-.20974	-.25928	-.03176	+1.235	+.1515
14	-.199	+.00041	-.00895	+.00497	-.20257	-.29558	-.03414	+1.460	+.1685

TABLE III

RUN # 1528 TABLE IV

POINT	.06 dn	.043 dδ	.355 n	.147 δ	υ	∫n	∫δ	∫n/υ	∫δ/υ
2	-.00814	-.00905	+.00708	-.00566	-.01577	+.000744	-.00137	-.0472	+.087
3	-.0518	0	-.0052	-.00633	-.06233	+.00113	-.00372	-.01814	+.0597
4	-.0554	0	-.0250	-.00633	-.08673	-.001234	-.00611	+.01423	+.0705
5	-.0554	0	-.0463	-.00637	-.10807	-.006846	-.00852	+.063	+.0787
6	-.0554	0	-.0670	-.00637	-.12877	-.015708	-.01093	+.1222	+.0851
7	-.0483	0	-.0873	-.00637	-.14197	-.02789	-.01334	+.1968	+.0943
8	-.0402	0	-.1048	-.00637	-.15137	-.04296	-.01575	+.283	+.104
9	-.0315	0	-.1174	-.00637	-.15527	-.0603	-.01816	+.388	+.1168
10	-.0264	0	-.128	-.00637	-.16077	-.0794	-.02057	+.496	+.128
11	-.0173	0	-.136	-.00637	-.15967	-.10012	-.02299	+.628	+.1437
12	-.01627	0	-.1422	-.00637	-.16484	-.1219	-.02539	+.74	+.154
13	-.01017	0	-.143	-.00637	-.15945	-.1446	-.0278	+.906	+.1745
14	-.00305	0	-.15	-.00637	-.15942	-.168	-.03021	+1.052	+.1897
15	+.00235	0	-.1505	-.00637	-.15452	-.1915	-.03262	+1.24	+.2115
16	+.00508	0	-.147	-.00637	-.14829	-.238	-.03744	+1.604	+.2525
17	+.00763	0	-.1403	-.00637	-.13904	-.283	-.04226	+2.037	+.303
18	+.00915	0	-.1339	-.00637	-.13112	-.326	-.04708	+2.485	+.359

TABLE IV

RUN #1640 TABLE V

POINT	.3164n	.0242dδ	.136δ	.0441dn	v	Σn	Σδ	Σn/v	Σδ/v
2	+.0094	-.01993	-.008	-.02315	-.04168	+.00215	-.00268	-.0518	+.0643
3	-.01283	+.001836	-.00891	-.0648	-.0847	+.00189	-.00653	-.0223	+.0771
4	-.0436	+.00135	-.00846	-.0751	-.1258	-.00341	-.01020	+.0216	+.0811
5	-.0752	+.00119	-.00815	-.0657	-.1479	-.01445	-.01369	+.0977	+.0925
6	-.1008	+.00096	-.00793	-.0466	-.1544	-.03075	-.01704	+.199	+.1104
7	-.1238	+.00056	-.00770	-.0456	-.1765	-.0514	-.02033	+.291	+.1151
8	-.1400	+.00048	-.00755	-.02975	-.1768	-.0754	-.02355	+.427	+.1331
9	-.1486	+.00048	-.0074	-.01672	-.1722	-.1019	-.02610	+.591	+.1551
10	-.1538	+.00034	-.00725	-.0064	-.1671	-.1296	-.02975	+.775	+.178
11	-.1557	+.00042	-.0071	+.00114	-.1582	-.1580	-.0328	+.998	+.207
12	-.1513	+.00040	-.0071	+.0128	-.1452	-.1859	-.03585	+1.28	+.247

RUN #1652 TABLE VI

POINT	.3418n	.0486dδ	.286dδ	.0467dn	v	Σn	Σδ	Σn/v	Σδ/v
2	+.00529	+.00059	-.0114	-.0379	-.04342	+.00256	-.00262	-.0591	+.0604
3	-.02855	+.00206	-.011	-.0580	-.09549	+.00069	-.0056	-.00726	+.0587
4	-.0651	+.00251	-.0099	-.0580	-.13047	-.00815	-.0083	+.0625	+.0636
5	-.1014	+.00199	-.0088	-.0580	-.16626	-.02375	-.01071	+.1428	+.0644
6	-.1311	+.00077	-.0082	-.0400	-.17854	-.0456	-.01293	+.255	+.0724
7	-.1522	+.00041	-.0079	-.0318	-.19155	-.0722	-.01508	+.377	+.0787
8	-.1673	+.00041	-.0078	-.0168	-.19350	-.1026	-.0171	+.530	+.0883
9	-.1740	+.00037	-.0076	+.00034	-.18094	-.1346	-.0191	+.743	+.1055
10	-.1701	+.00037	-.0076	+.00684	-.17045	-.1668	-.02105	+.978	+.1235
11	-.1653	+.00037	-.0074	+.00694	-.16550	-.1981	-.023	+1.195	+.1340
12	-.1603	+.00022	-.0075	+.00684	-.16099	-.2285	-.02485	+1.420	+.1545

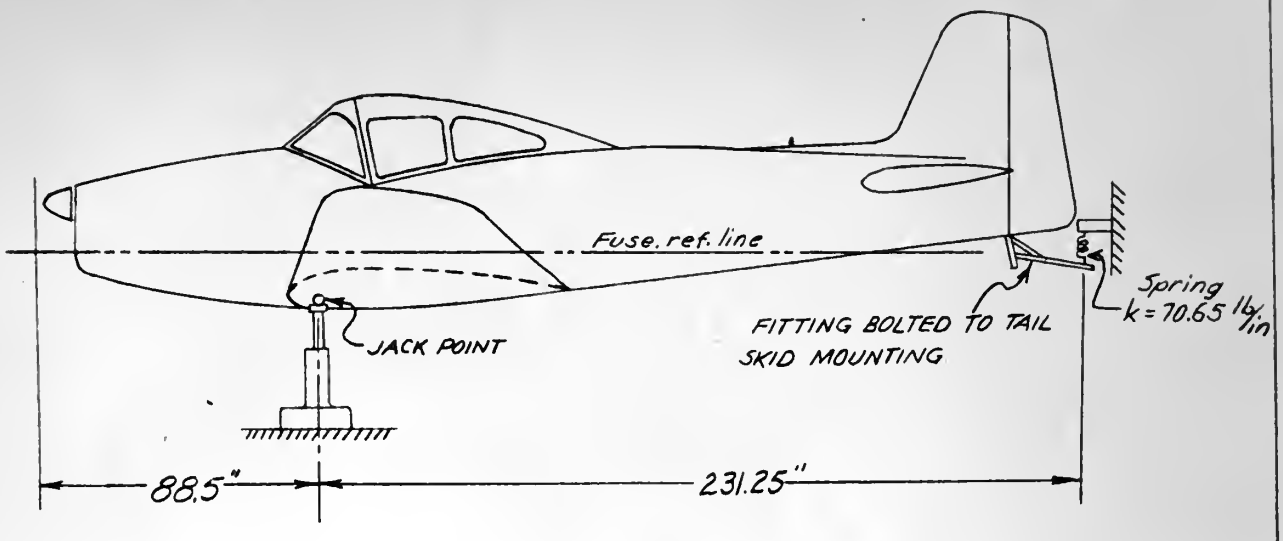

FIG. 1

DETERMINATION OF MOMENT OF INERTIA

Assuming an undamped oscillation, then

$$I = \frac{P^2 K}{4\pi^2}$$

P = 0.618 seconds (Period)
K = 314,000 ft lb

I = 3055 SLUG FT^2 ABOUT JACK POINTS

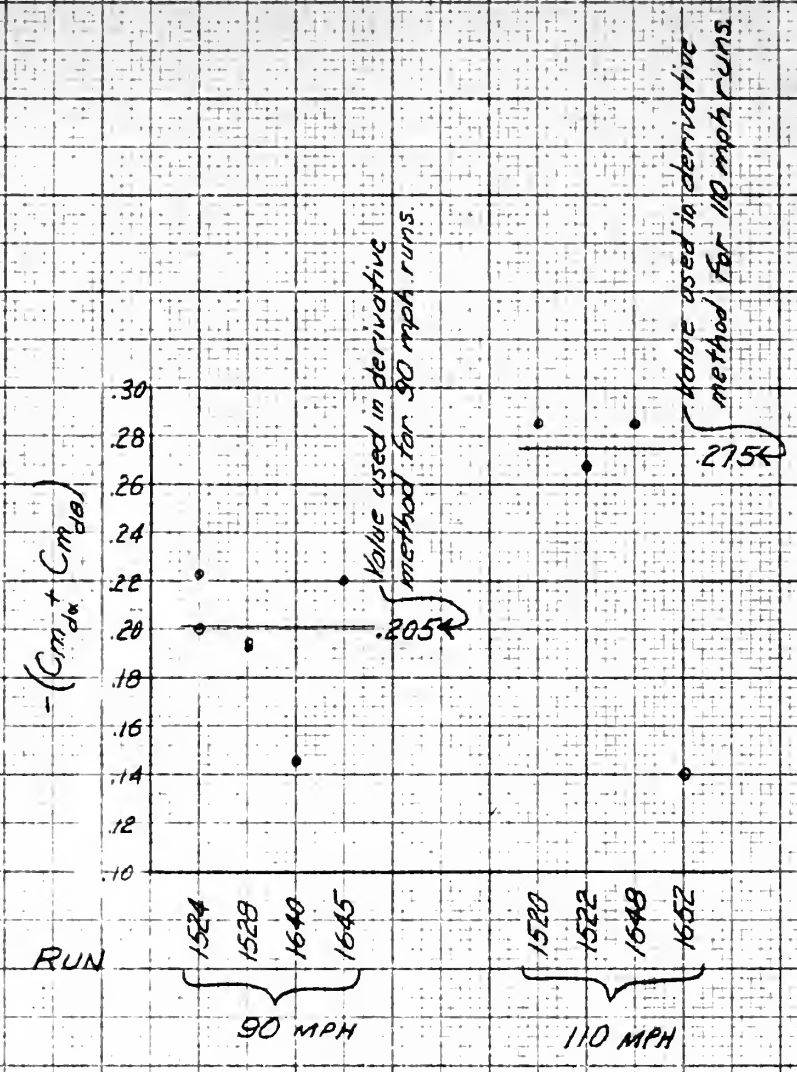

Fig 2

Showing values of $-(Cm_{d\alpha}+Cm_{dq})$ obtained from the various runs by the equations of motion method of data reduction. The value used for $-(Cm_{d\alpha}+Cm_{dq})$ in the derivative method is also indicated.

PLOT OF DATA FOR

$$\frac{L\int n\,d\frac{y}{v}}{v} + \frac{M\int \delta\,d\frac{y}{v}}{v} = 1$$

RUN #1528

$L = \frac{1}{.697} = 1.435$

RUN #1640

$L = \frac{1}{.537} = 1.73$

BOTH RUNS 90 mph

$M = \frac{1}{.073} = 13.33$

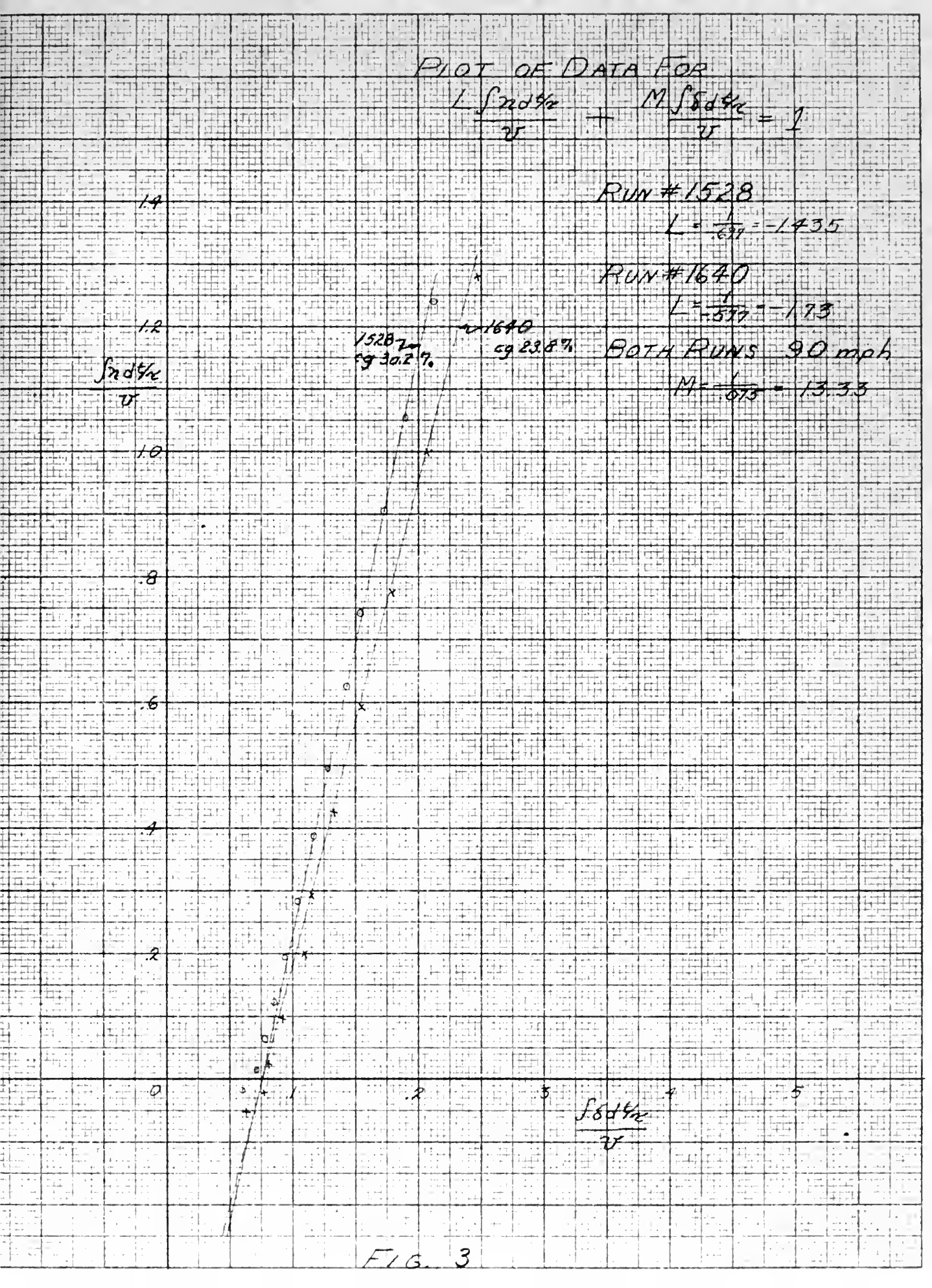

FIG. 3

PLOT OF DATA FOR

$$L\frac{\int n\,d\psi_x}{v} + M\frac{\int \delta\,d\psi_x}{v} = 1$$

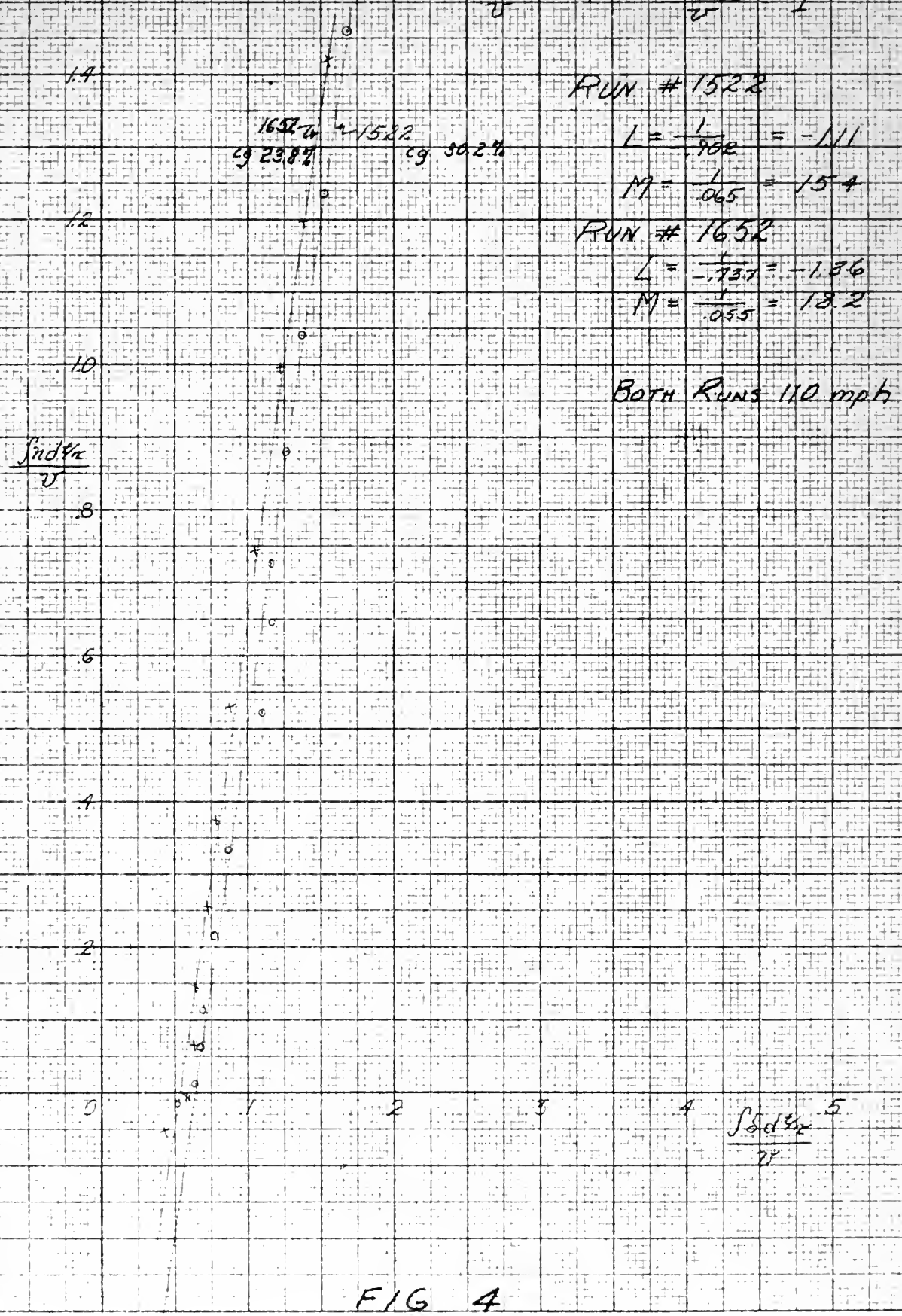

RUN # 1522

$L = \frac{1}{-.900} = -1.11$

$M = \frac{1}{.065} = 15.4$

RUN # 1652

$L = \frac{1}{-.737} = -1.36$

$M = \frac{1}{.055} = 18.2$

BOTH RUNS 110 mph

FIG 4

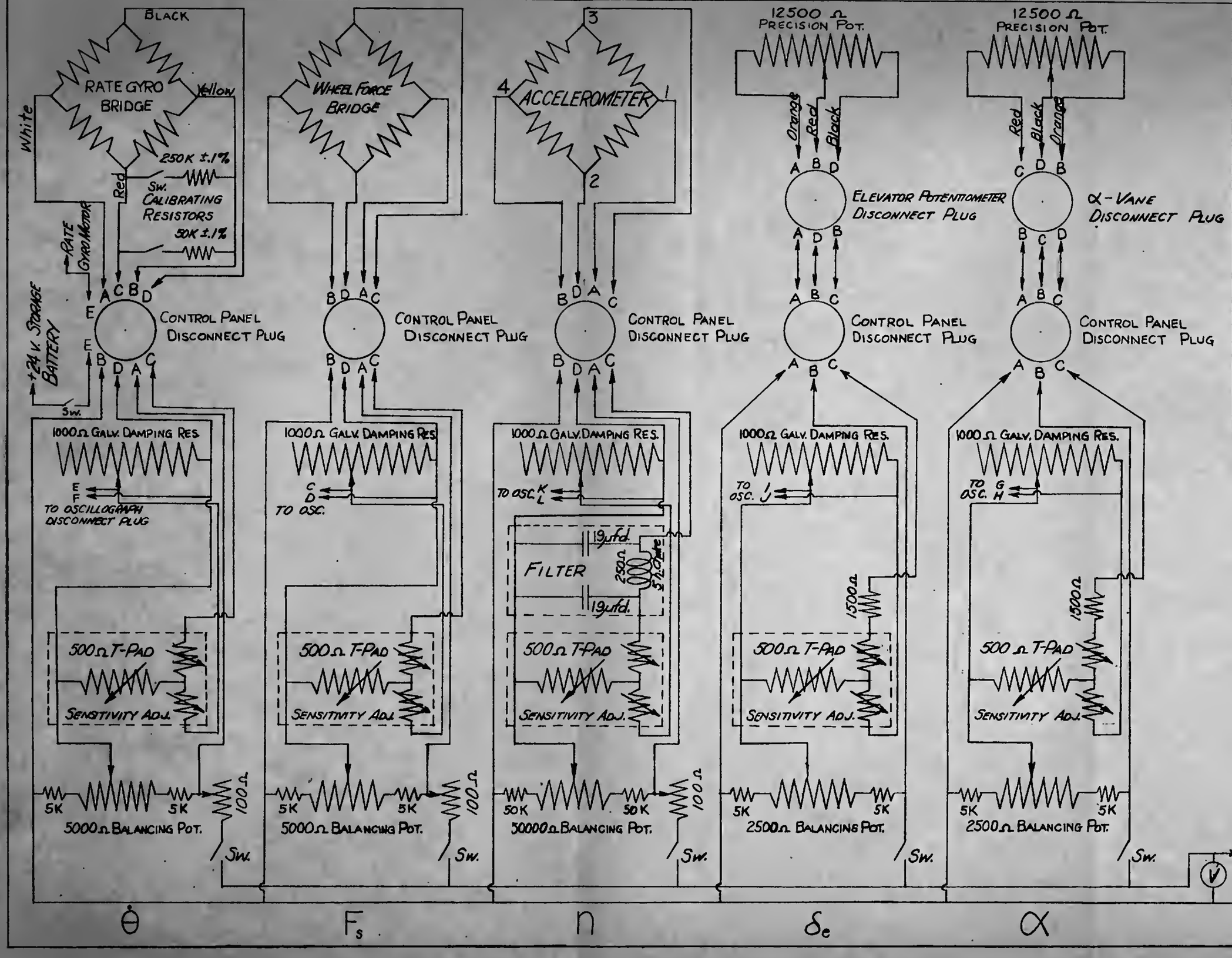

Fig. 5
WIRING DIAGRAM
OF
INSTRUMENTATION SYSTEM
FOR DYNAMIC FLIGHT TESTING OF
RYAN NAVION. N5113K.

J. Firmin

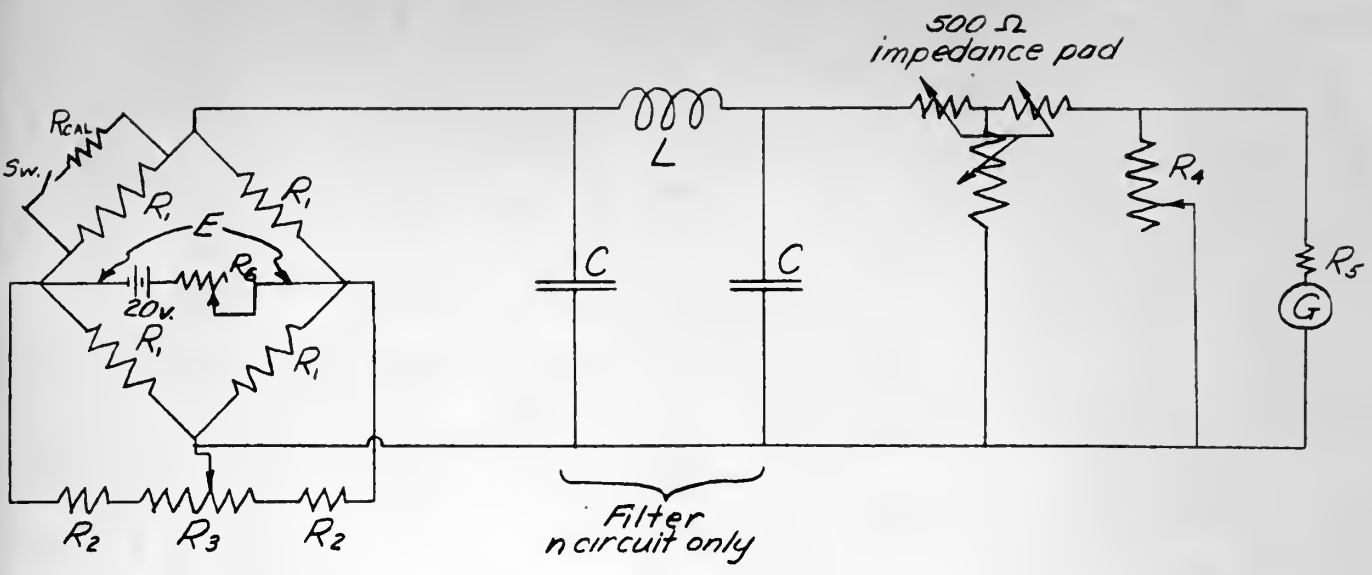

E 18 v. for n-circuit. 15 v. for F_s and $\dot{\theta}$ circuits.
R_1 120 Ω. SR-4 strain guages in F_s and $\dot{\theta}$ circuits
8435 Ω strain guages in n circuit
R_2 50,000 Ω current limiting resistors - n circuit
5000 Ω do do do F_s and $\dot{\theta}$ circuits
R_3 50,000 Ω balancing potentiometer, n circuit
5000 Ω do do F_s and $\dot{\theta}$ circuit
R_4 1000 Ω galvanometer damping resistor

R_5 26.5 Ω resistance of galvanometer
R_6 100 Ω voltage adjusting resistors
R_{CAL} 50K and 250K, ± 0.1% calibrating resistors
$\dot{\theta}$ circuit only
L 250 Ω, 5 henry inductance
C 19 μfd capacitor
G Oscillograph galvanometer

Fig. 6

SCHEMATIC CIRCUIT DIAGRAM FOR PITCH RATE, STICK FORCE, a_n AND NORMAL ACCELERATION CIRCUITS.

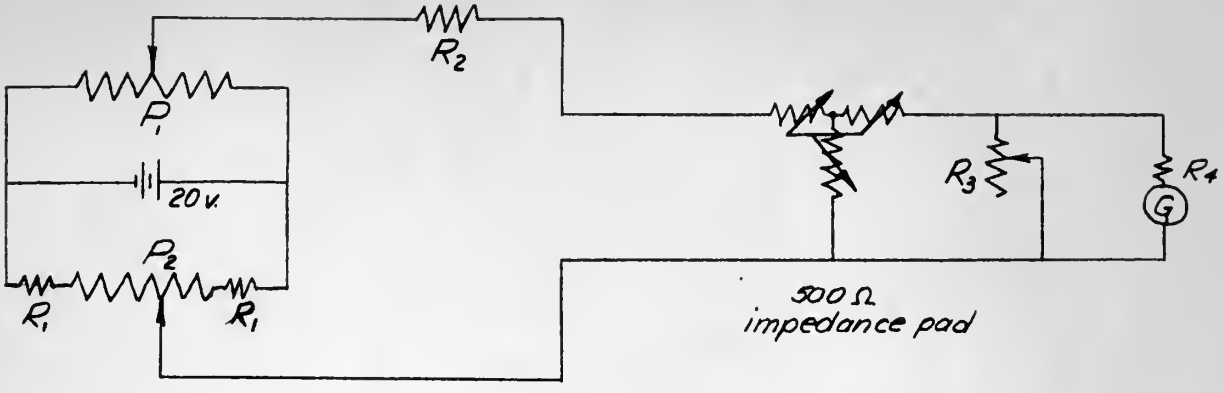

P_1 12500Ω precision potentiometer. Sensing α or δ_e
P_2 2500Ω balancing potentiometer.
R_1 5000Ω current limiting resistor
R_2 1500Ω load resistor
R_3 1000Ω galvanometer damping resistor
R_4 26.5Ω resistance of galvanometer
G Oscillograph galvanometer

Fig. 7

SCHEMATIC CIRCUIT DIAGRAM FOR ANGLE OF ATTACK $^{\alpha}n_d$ ELEVATOR ANGLE CIRCUITS.

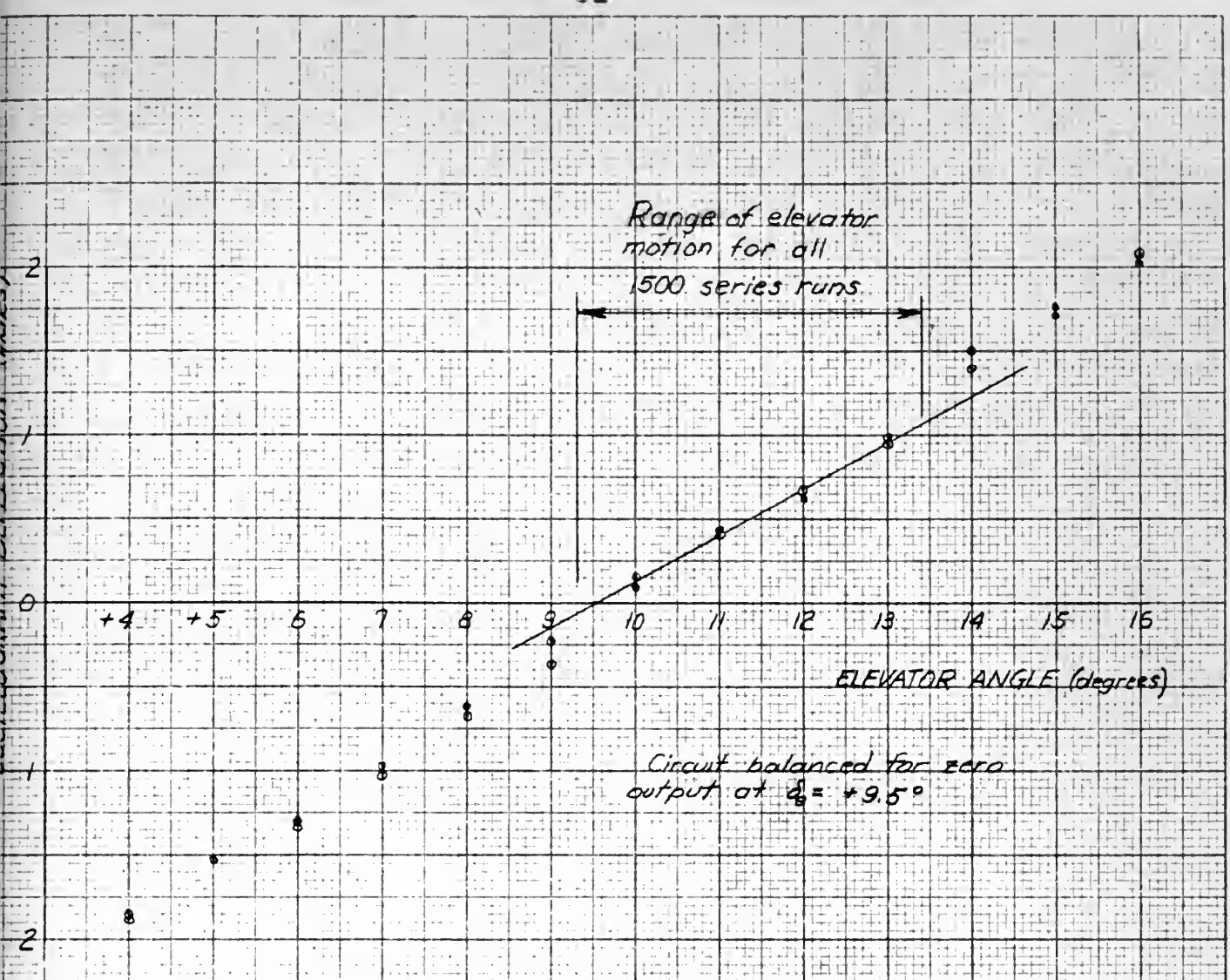

Fig 8

ELEVATOR DEFLECTION ANGLE CALIBRATION for "1500" SERIES RUNS

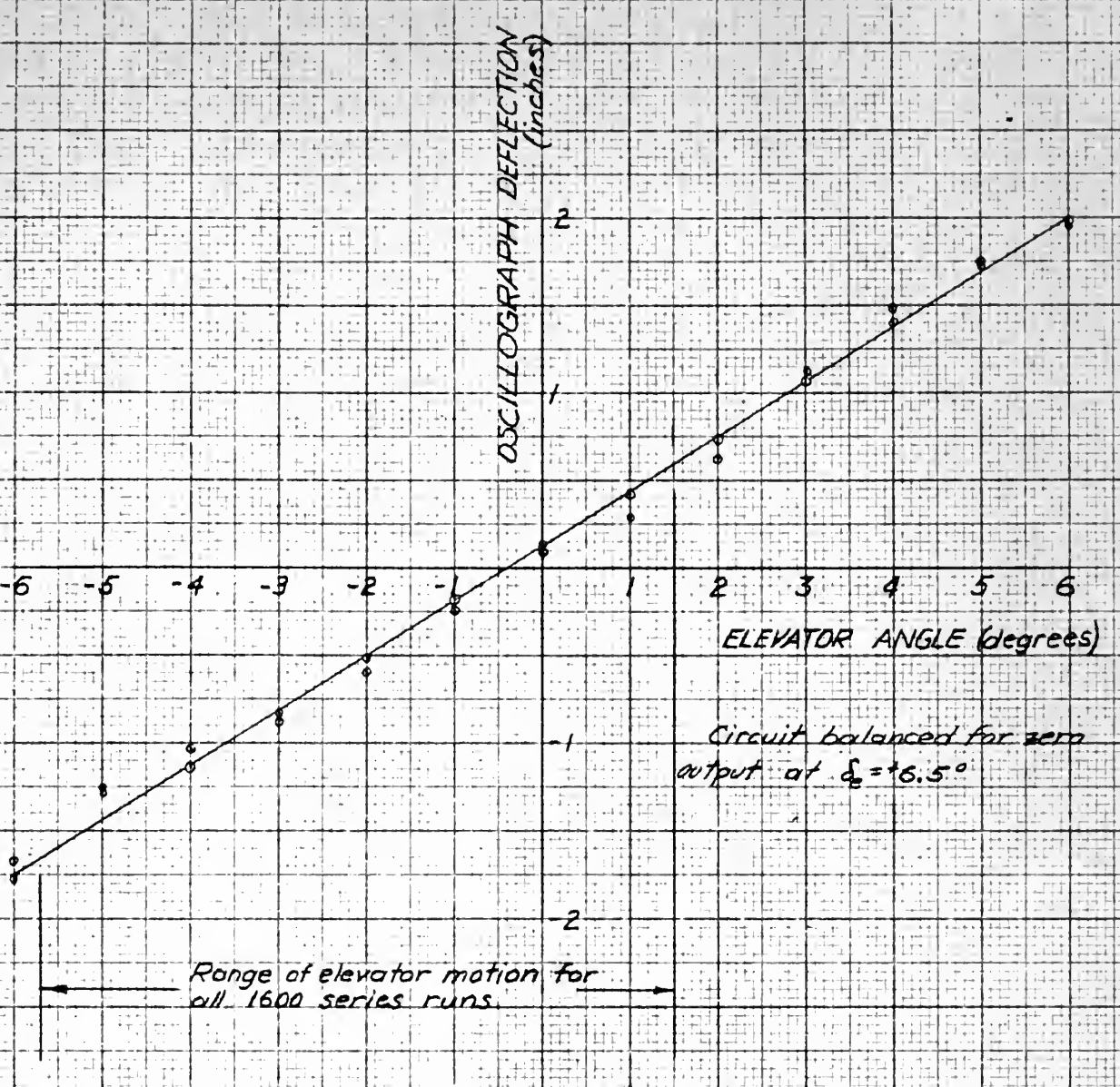

Fig. 9

ELEVATOR DEFLECTION ANGLE CALIBRATION for "1600" SERIES RUNS

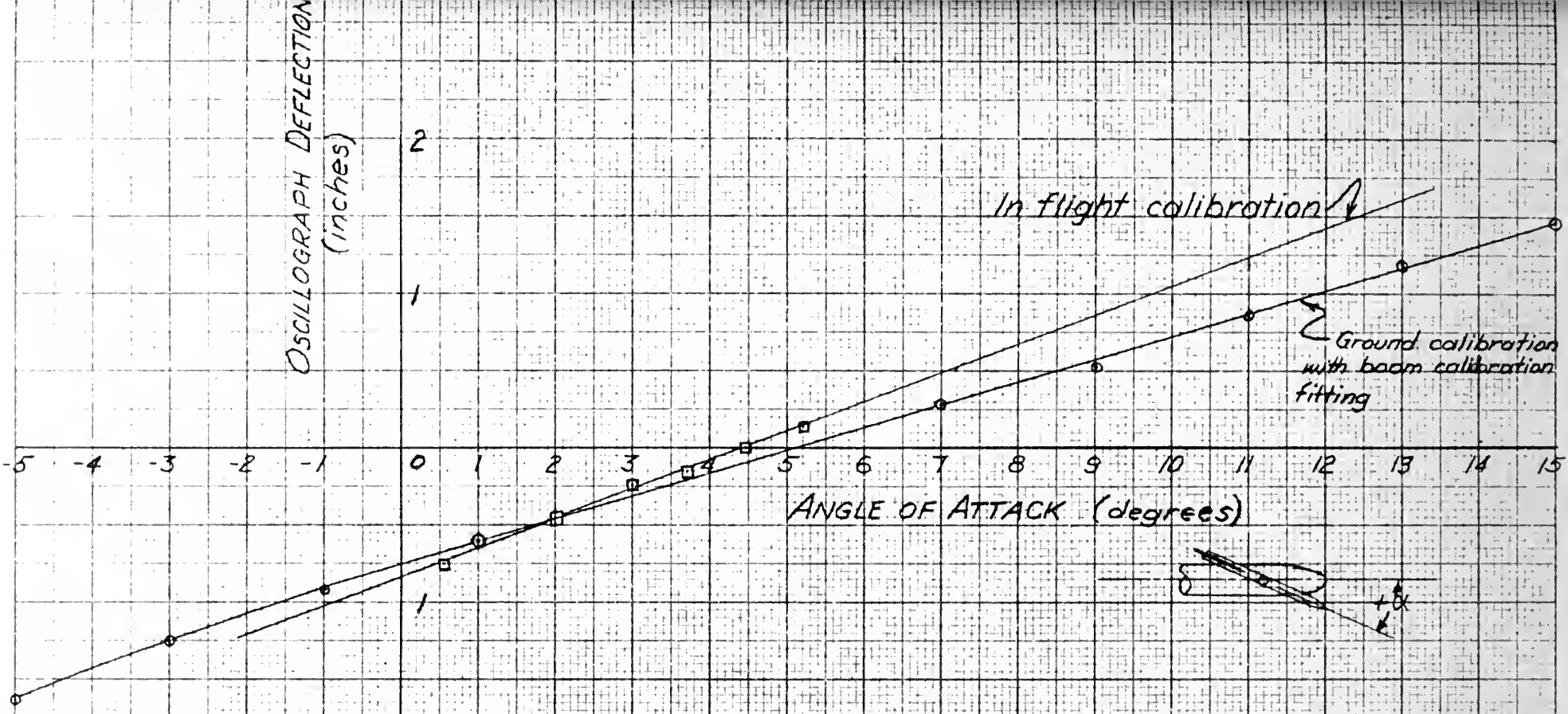

FIG. 10

ANGLE OF ATTACK CALIBRATION
"1500" Series Runs

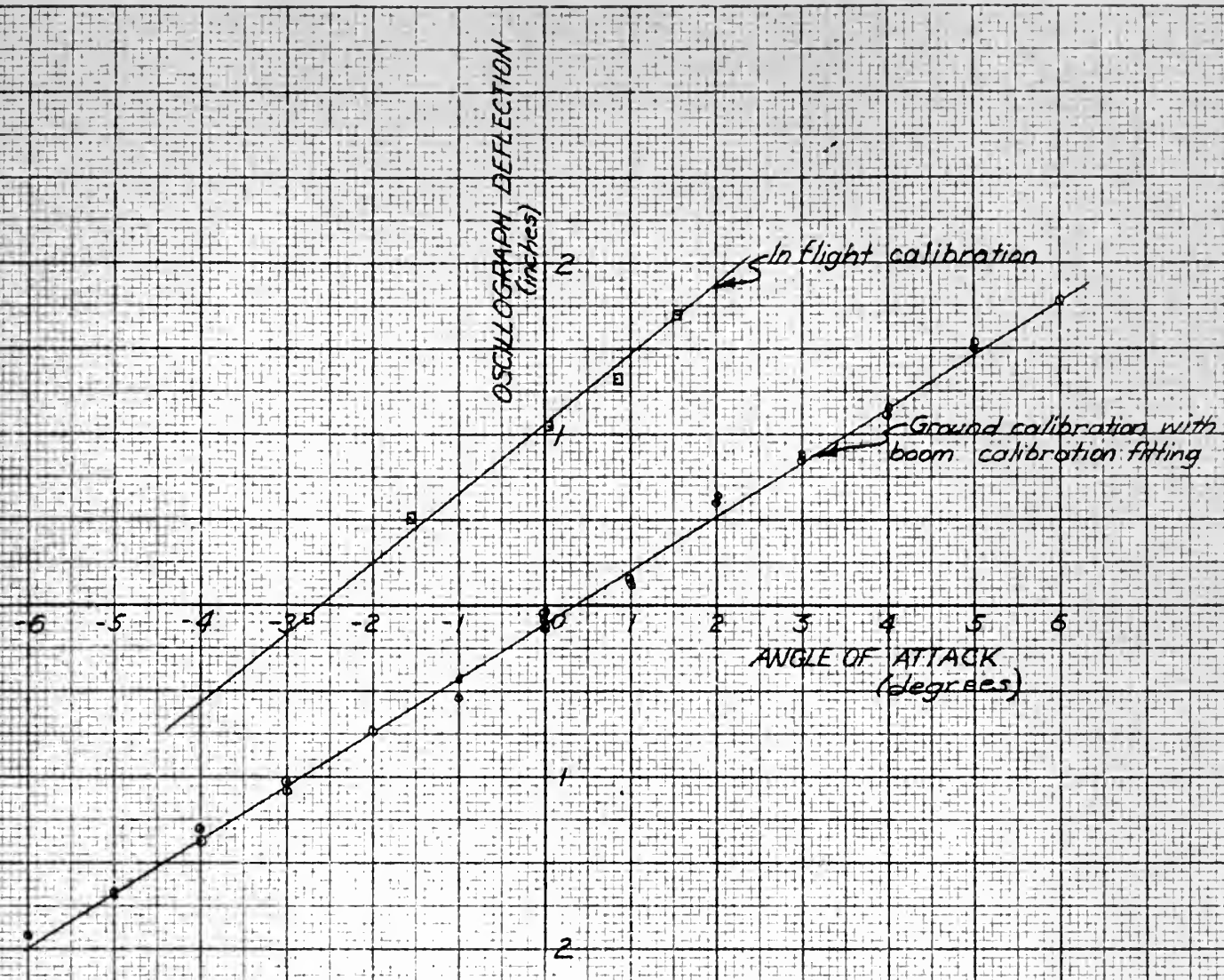

Fig 11

ANGLE OF ATTACK CALIBRATION
for
"1600" SERIES RUNS

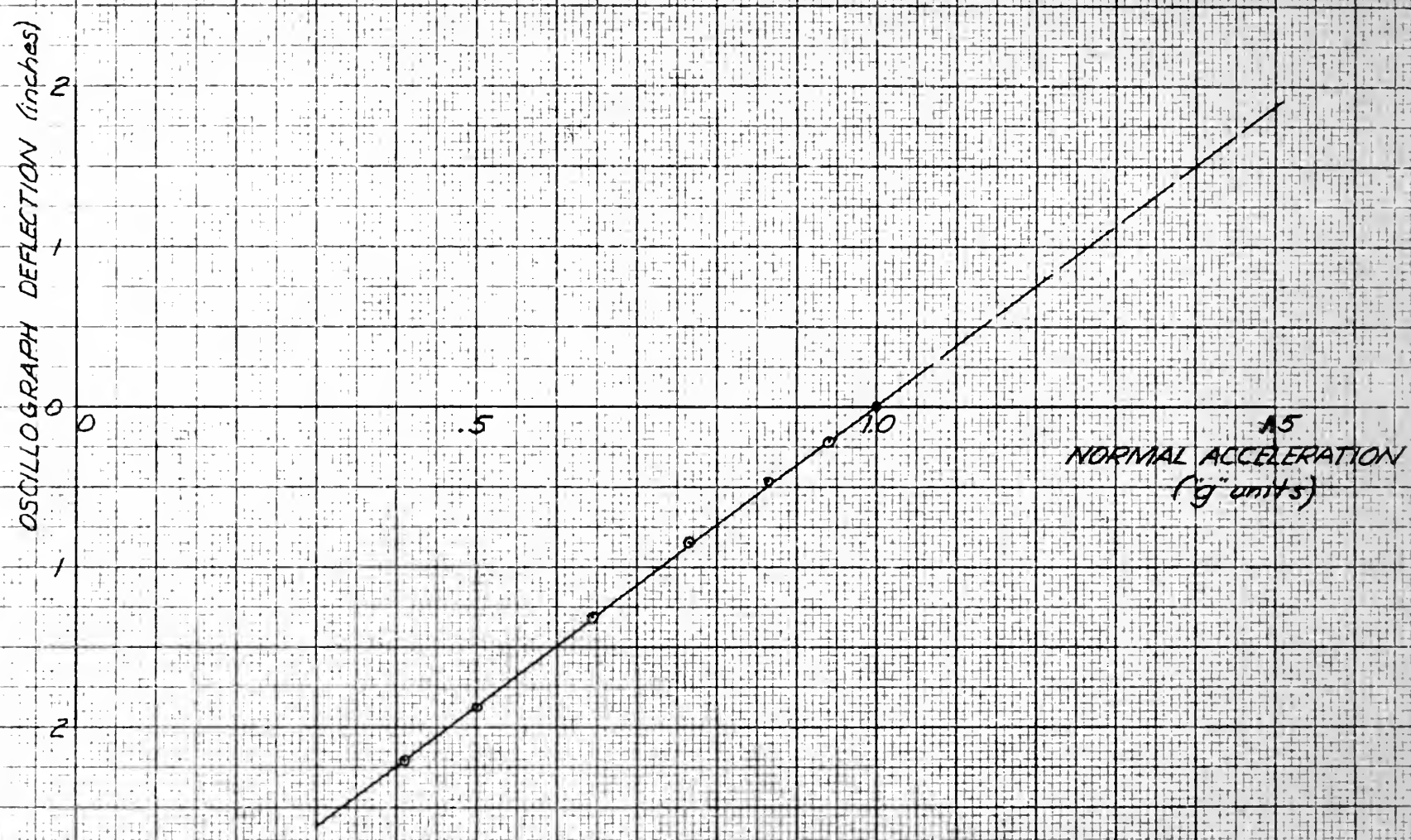

Fig 12

ACCELEROMETER CALIBRATION

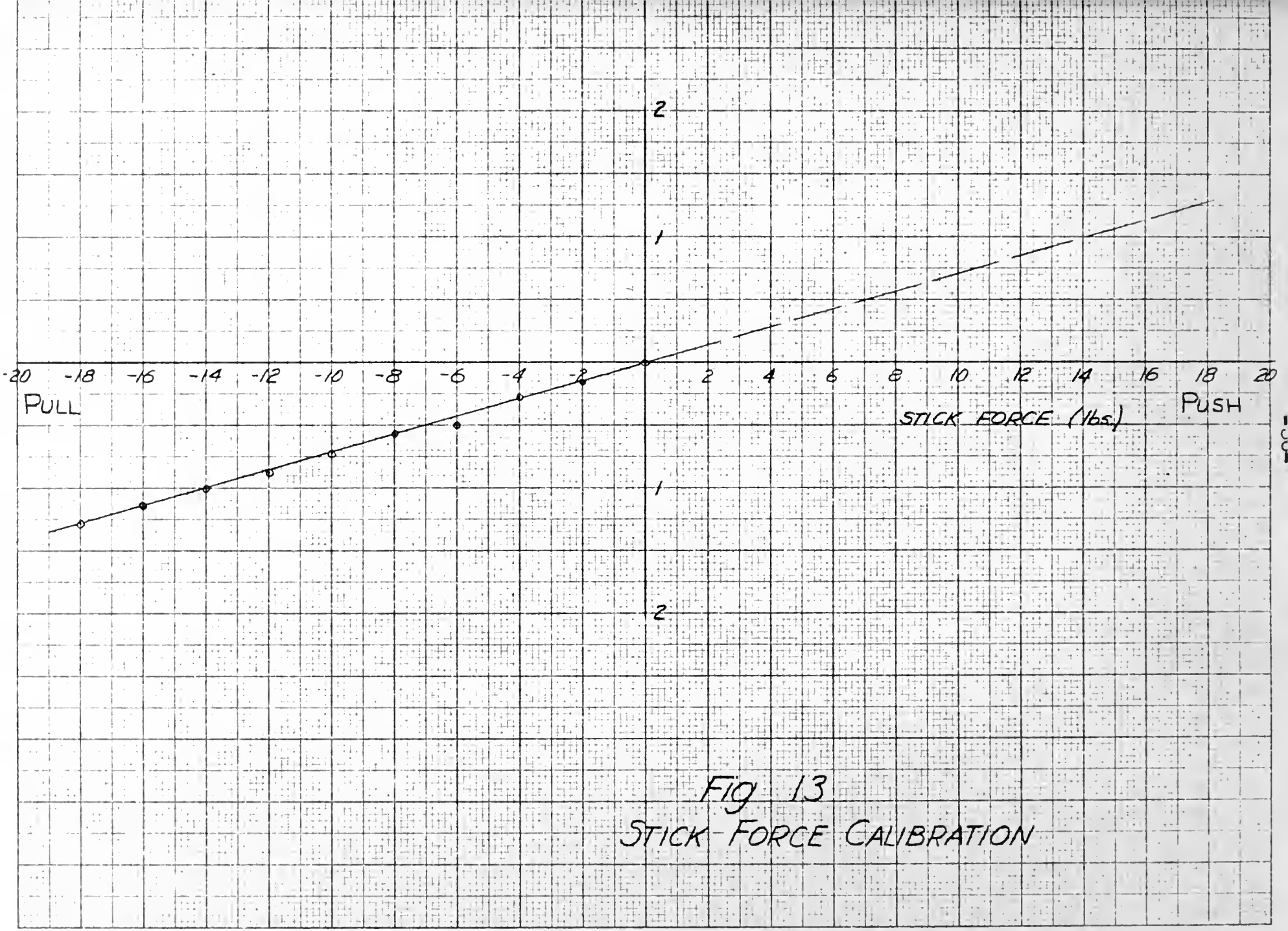

Fig 13
STICK FORCE CALIBRATION

PENDULUM CALIBRATION OF PITCH RATE GYRO

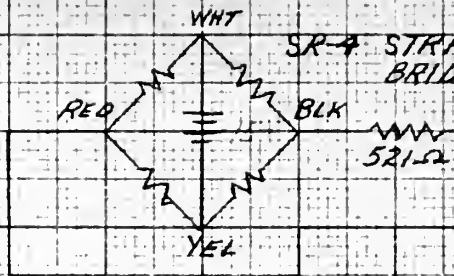

SR-4 STRAIN GAGE BRIDGE

521Ω

G 27Ω

CONSOLIDATED ENG. GALVANOMETER 12.5 μa/in

R-CAL CONNECTED RED TO YEL

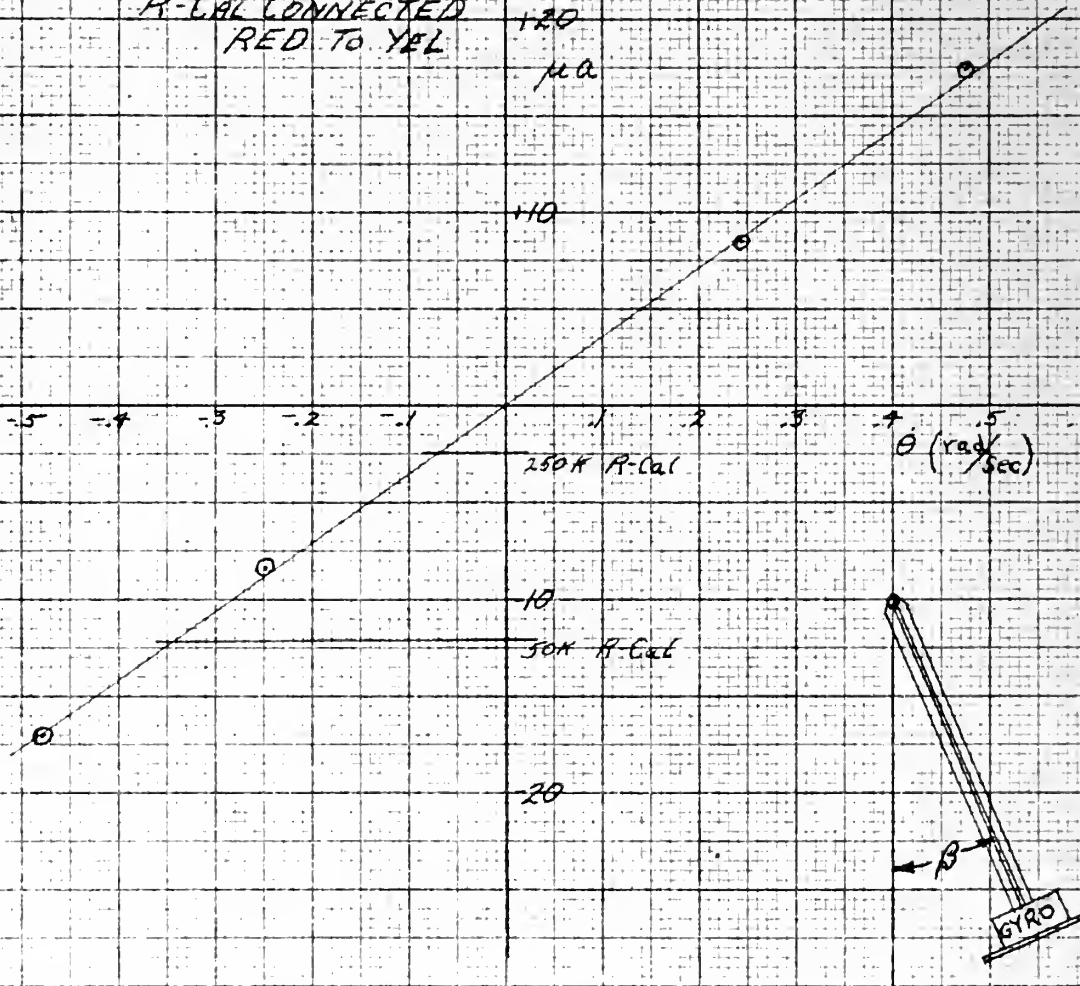

$$\dot{\theta}_{MAX} = \sqrt{\frac{8\pi^2}{T^2}(1-\cos\beta)}$$

where T = Period in seconds

PENDULUM ARRANGEMENT

FIG. 14

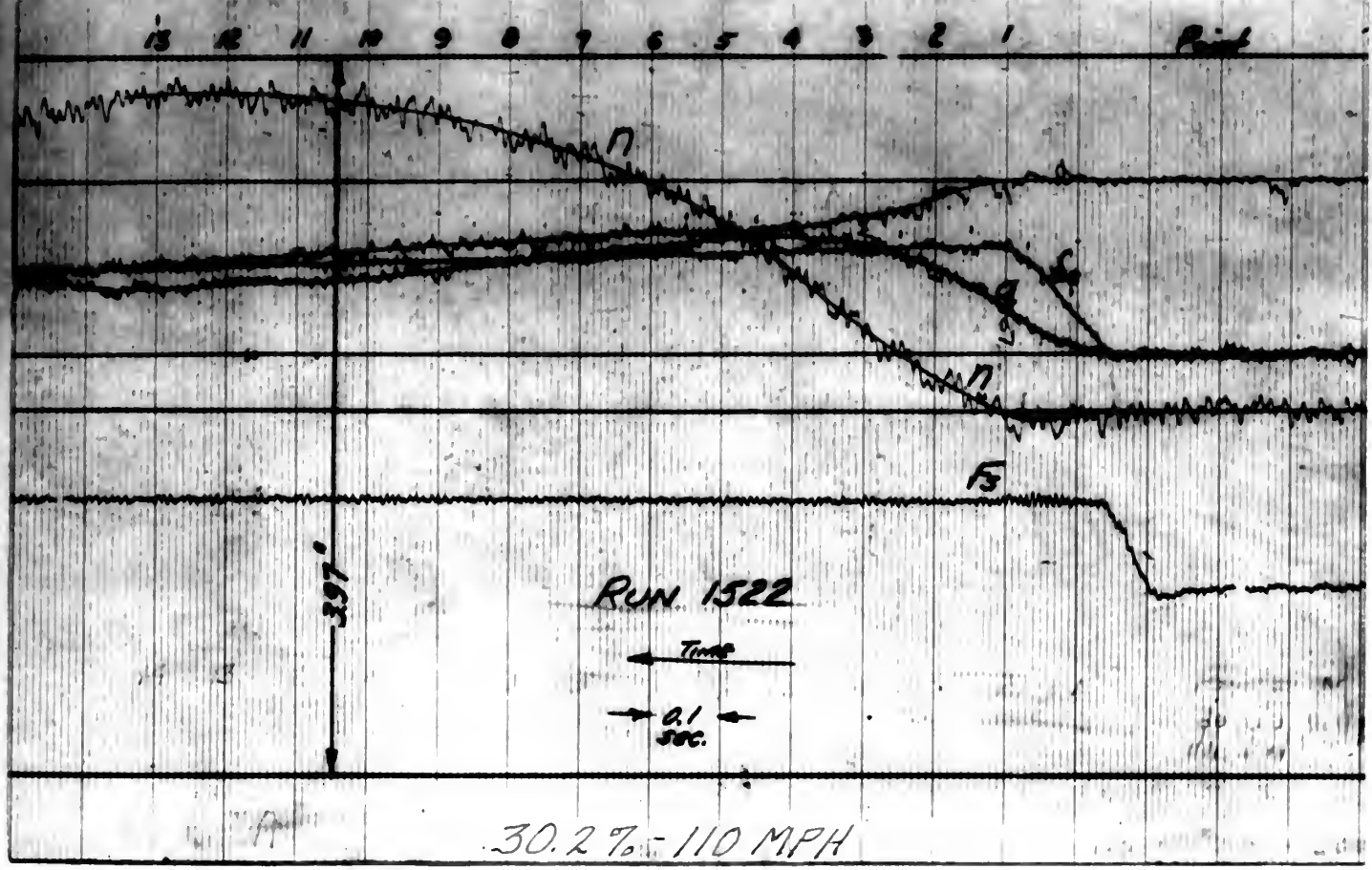

30.2% - 110 MPH

FIG. 15

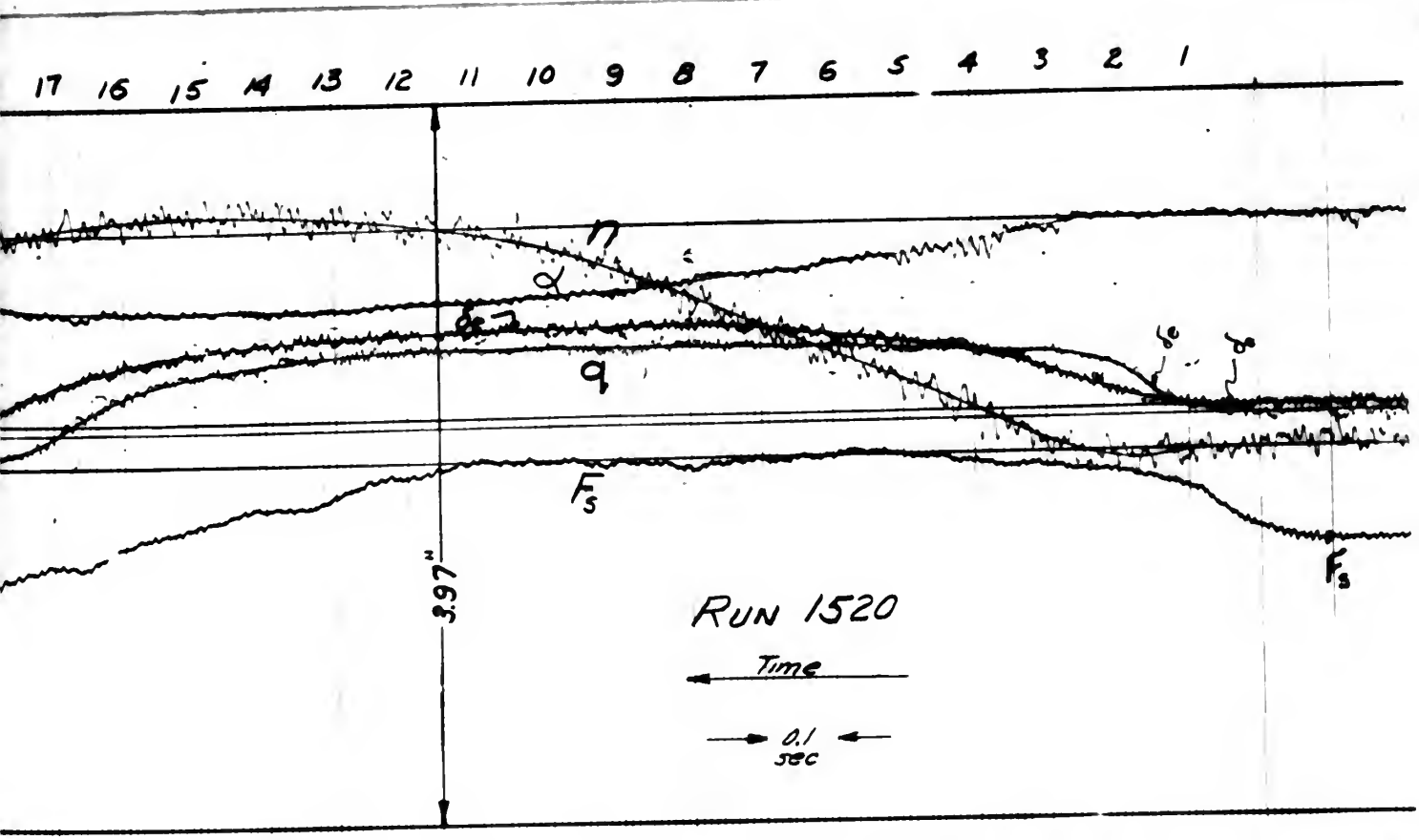

Aft c.g. 30.2% PULSE δe INPUT - 110 MPH - 4900' - 10°C 1850 RPM

FIG. 16

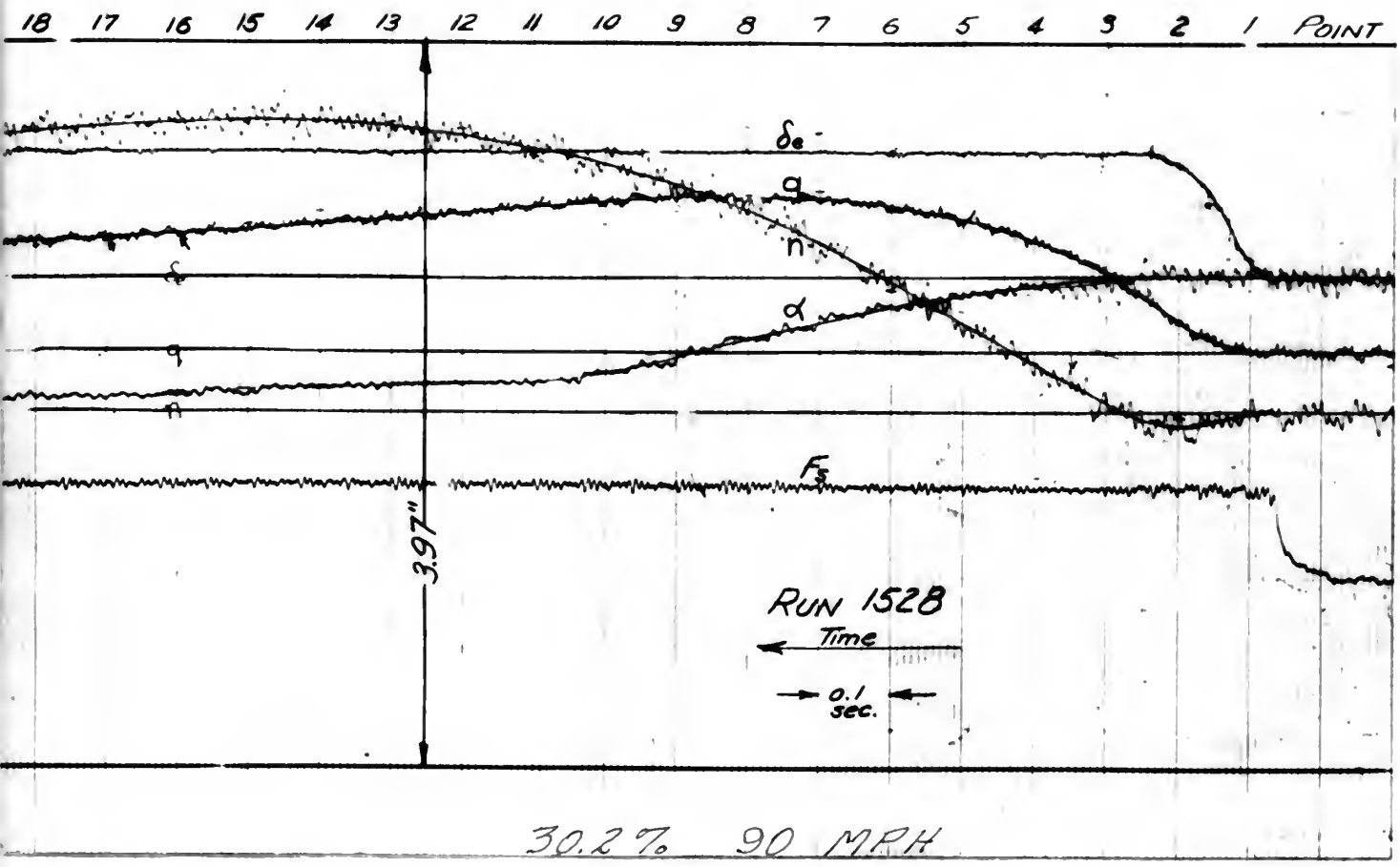

30.27. 90 MPH

FIG. 17

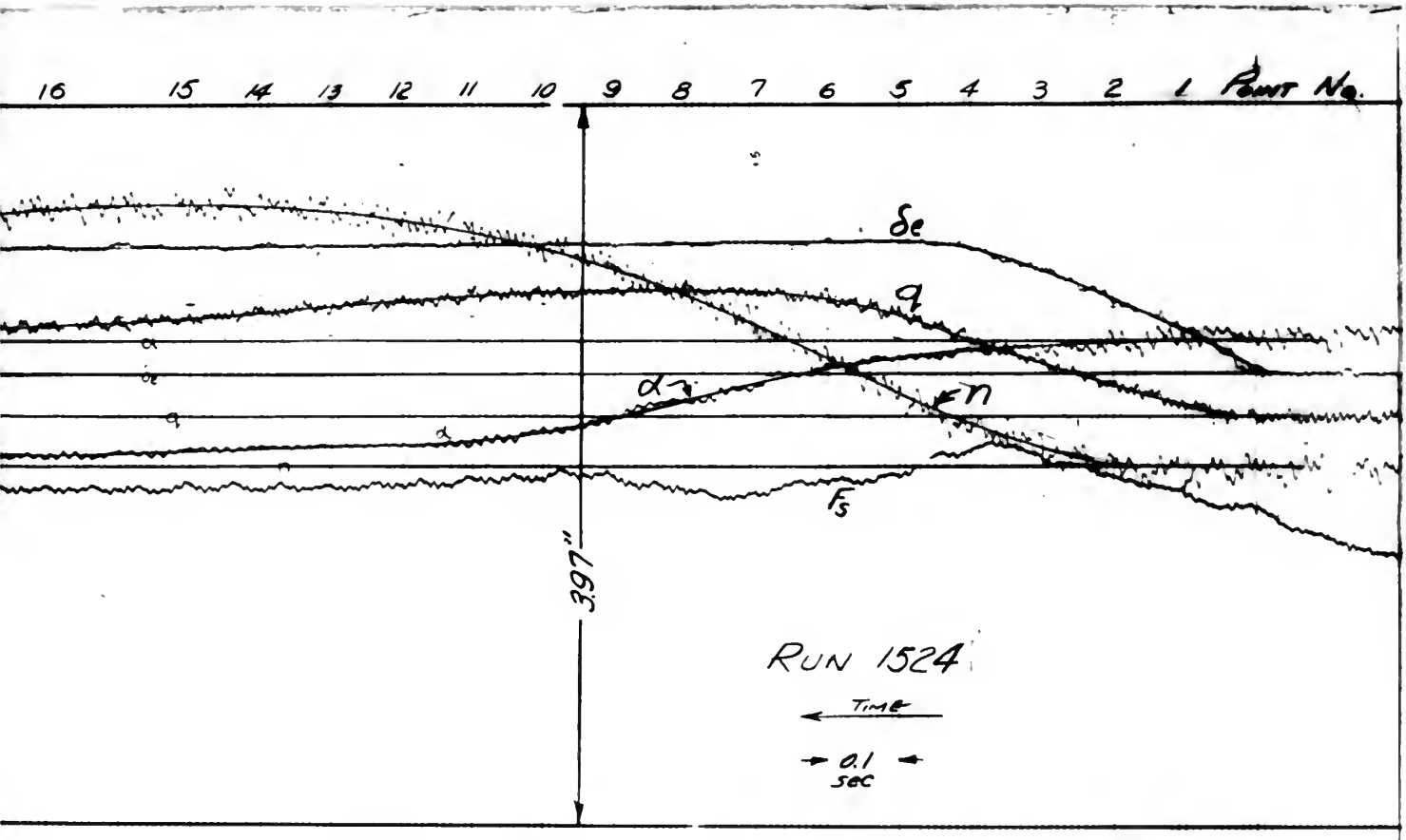

30.27. STEP δe INPUT - 5600' - 90 MPH - 1800 RPM - 16" - 3°C

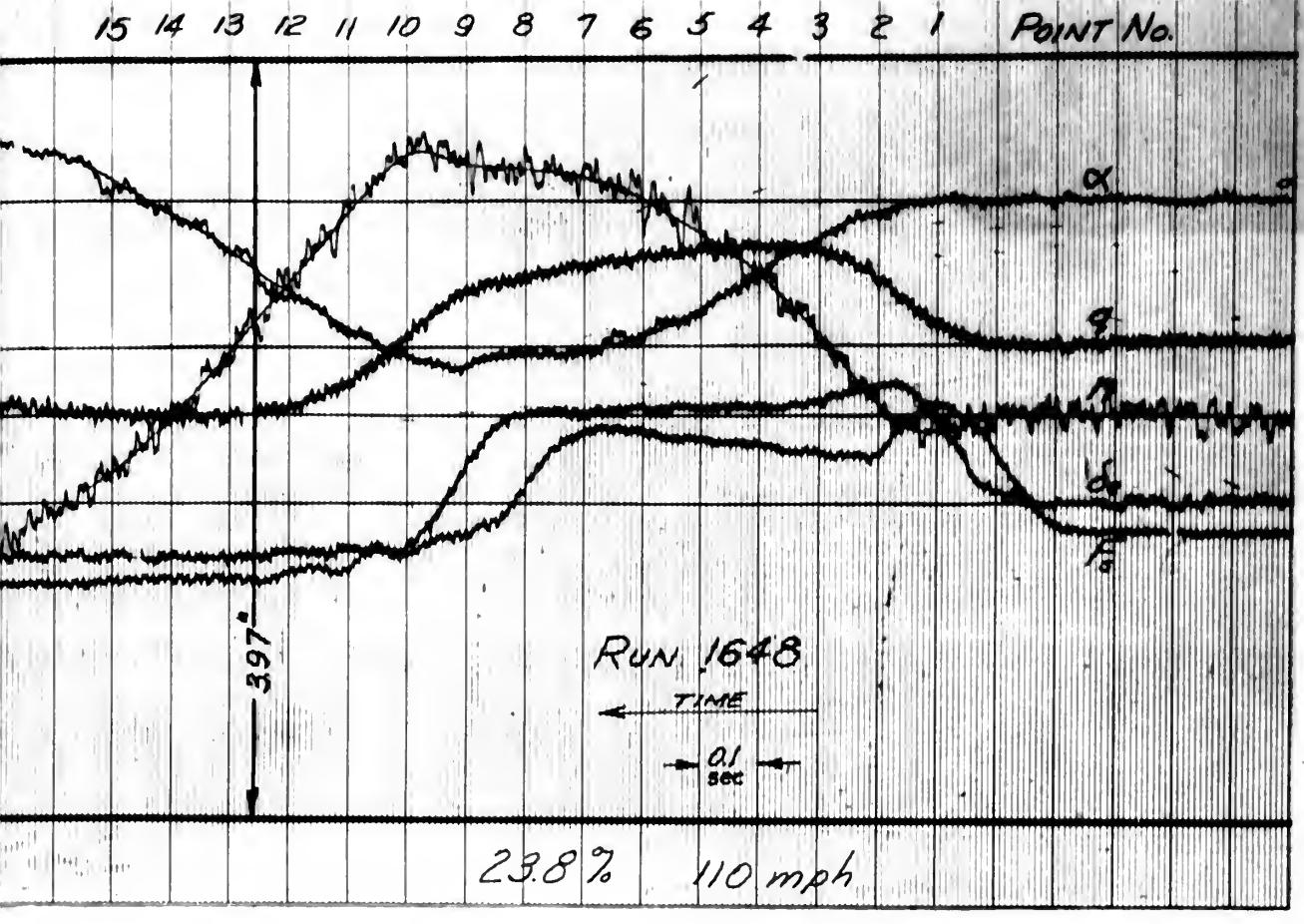
15 14 13 12 11 10 9 8 7 6 5 4 3 2 1 POINT No.
α
q
η
δe
F3
.397"
RUN 1648
TIME
0.1 sec
23.8% 410 mph

FIG 19

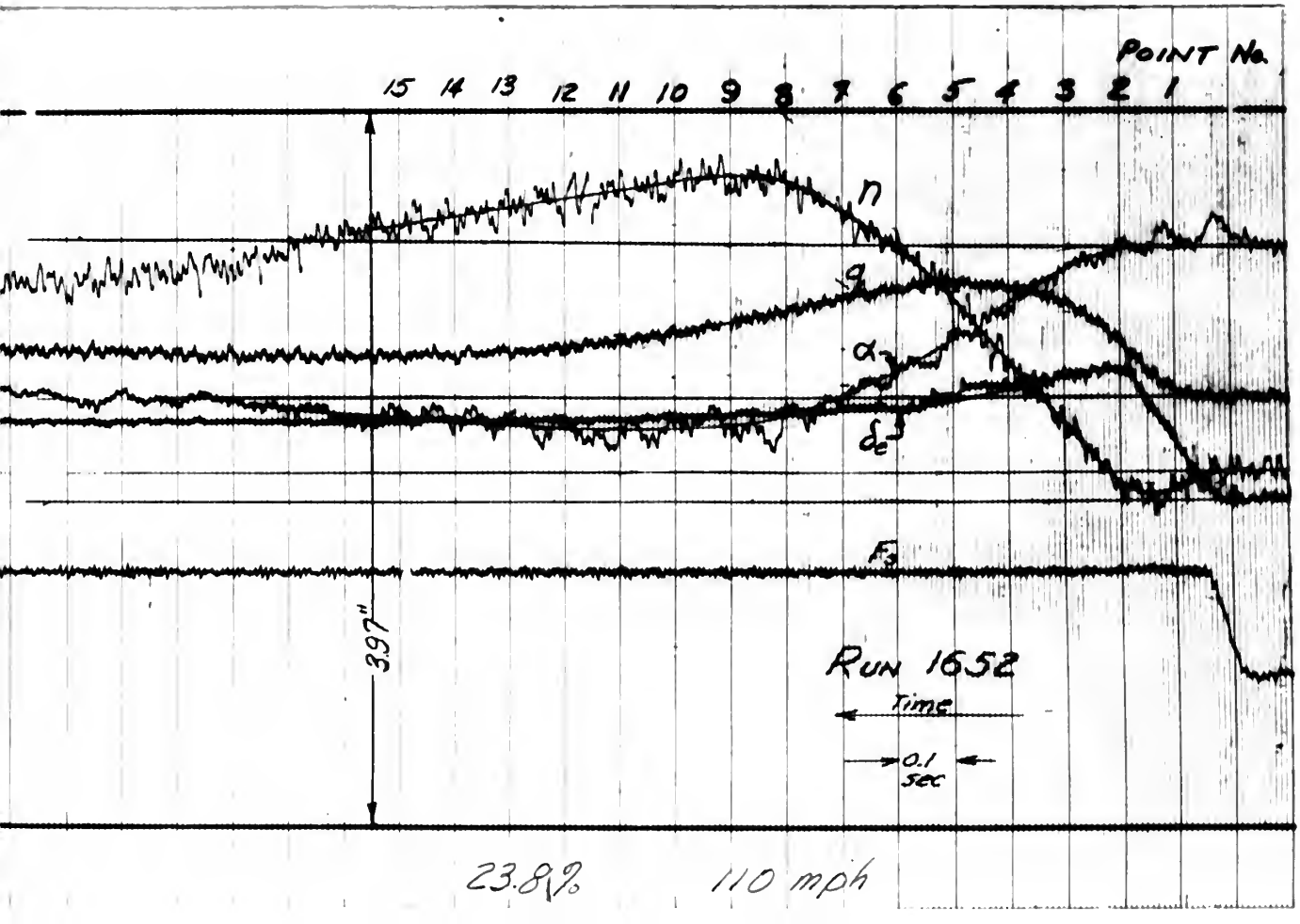
POINT No.
15 14 13 12 11 10 9 8 7 6 5 4 3 2 1
η
q
α
δe
F3
.397"
RUN 1652
Time
0.1 sec
23.8% 410 mph

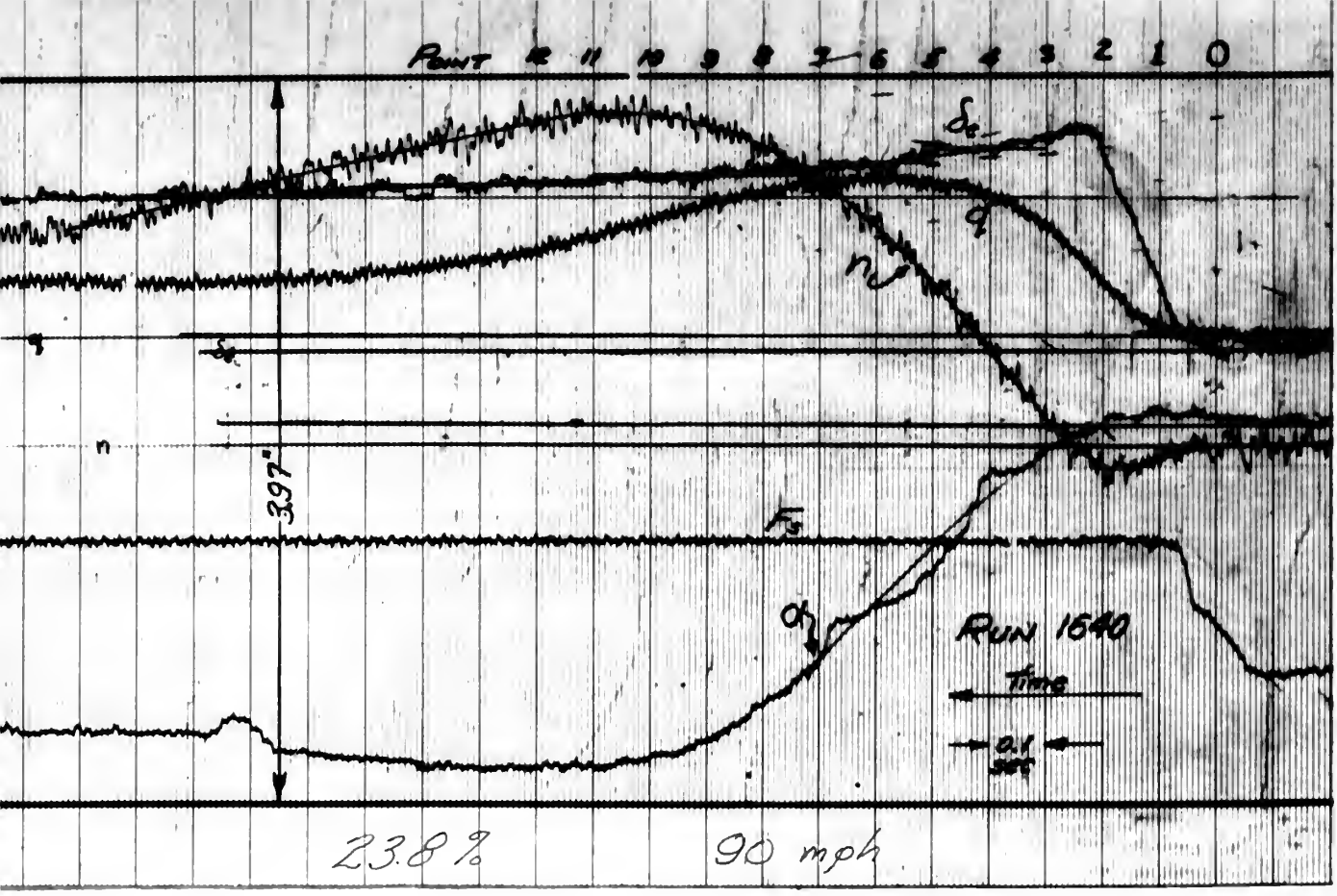

23.8% 90 mph

FIG 21

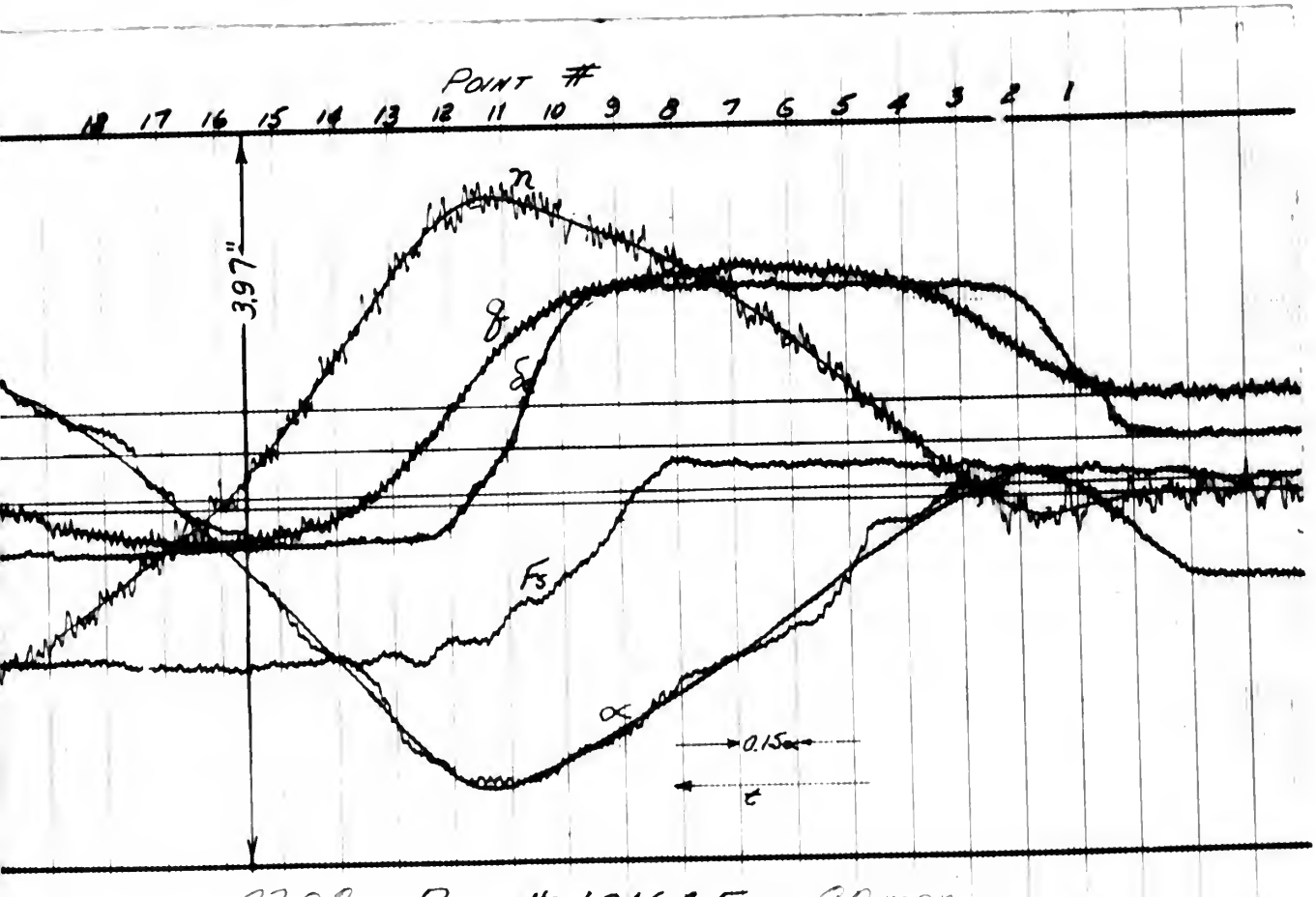

23.8% RUN #101645 90 mph